

# Chapter 6

## Theoretical Analysis of Electron Transfer in Proteins: From Simple Proteins to Complex Machineries

G. Matthias Ullmann<sup>a,\*</sup>, Lars Mueller<sup>a</sup>, and Elisa Bombarda<sup>b</sup>

<sup>a</sup>Structural Biology/Bioinformatics, University of Bayreuth,  
Universitätsstr. 30, NW I, 95447 Bayreuth, Germany

<sup>b</sup>Experimental Physics IV, University of Bayreuth, Universitätsstr.  
30, 95447 Bayreuth, Germany

Summary.....	99
I. Introduction.....	100
II. Theoretical Description of Electron Transfer Reactions.....	102
A. Marcus Theory of Electron Transfer.....	102
B. Electronic Coupling.....	104
C. Reorganization Energy.....	105
D. Reaction Free Energy.....	106
E. Moser-Dutton Ruler.....	106
F. Tuning of Electron Transfer Rates in Proteins.....	107
III. Electrostatic Methods for Estimating Reaction Free Energies and Reorganization Energies.....	108
A. The Poisson-Boltzmann Equation.....	108
B. Calculating the Outer Sphere Reorganization Energies.....	110
C. Calculating Redox Potentials of Proteins.....	111
D. Interacting Redox Active Groups.....	112
E. Looking at the Coupling of Reduction Reactions to Protonation Reaction.....	116
F. Influence of Membrane Potential and Transmembrane Gradients.....	117
IV. Complex Electron Transfer Proteins.....	120
A. Simulating Complex Electron Transfer Networks.....	120
B. Analyzing Calculated Electron Transfer Networks.....	121
C. Electron Transfer from the C-Subunit of the Photosynthetic Reaction Center to the Special Pair.....	121
V. Conclusions.....	122
Acknowledgements.....	125
References.....	125

### Summary

Electron transfer plays a central role in many biological processes such as, for instance, photosynthesis or oxidative phosphorylation, but also in other bioenergetic processes such as denitrification or sulfate and sulfite reduction. Moreover, electron transfer is a key step in

---

\*Author for correspondence, e-mail: [ullmann@uni-bayreuth.de](mailto:ullmann@uni-bayreuth.de)

many enzymatic reactions. The framework of Marcus theory provides the theoretical basis to describe the kinetics of these reactions. The parameters to calculate rate constants can be estimated using protein crystal structures. Namely, the electronic coupling is related to the edge-to-edge distance between the redox-active sites. The reaction free energy and the reorganization energy can be obtained, for instance, from continuum electrostatic calculations. However, to perform complicated tasks, proteins often combine many redox cofactors and couple the redox reactions to protonation reactions or conformational changes. Moreover, electron transfer proteins are often embedded in membranes, and thus membrane potential and concentration gradients influence the reactions. One approach to describe such complex systems is the so-called microstate model, in which each state of a system is represented by a vector in which each component defines the status of each site (for instance oxidized or reduced, protonated or deprotonated). On the basis of this microstate description, it is possible to calculate the thermodynamics and kinetics of a complex protein system. In this article, we will review the principle features of the microstate model and explain how the parameters of the microstate model can be calculated using continuum electrostatics. The microstate model provides the theoretical framework to go from molecular structures to the mechanism of complex protein machines.

## I. Introduction

Electron transfer reactions are central in many biological processes such as photosynthesis and oxidative phosphorylation, to name just the most prominent biochemical pathways. Additionally, electron transfer also plays a central role in biochemical pathways such as the nitrogen cycle and the sulfur cycle that are of geochemical relevance. In recent years, the biochemical electron transfer processes also raised an increased interest because of its use in microbial fuel cells (Logan 2008; Zhou et al. 2013). Electron transfer reactions are even possible candidates to be processes at the origin of life in hydrothermal vents where electron transfer reactions are driven by pH gradients (Martin et al. 2008). These reactions are in some respect just the reverse of the chemi-osmotic theory of Mitchell (1961) and may thus help to explain the origin of the non-equilibrium state that is characteristic for living organisms.

Considering the central role of redox reactions in biochemical systems, it is not surprising that the redox potential is tightly controlled in the cell (Banerjee 2008). In fact, there are several redox buffering systems in the cell that are interconnected through

various complex enzymatic systems. One of the most prominent biological redox buffers is glutathione, a tri-peptide which forms dimers through its thiol group upon oxidation (Deponte 2013). Glutathione functions as an antioxidant in plants, animals, fungi, and some bacteria and archaea and prevents harmful reactions which can be caused by reactive oxygen species such as free radicals and peroxides. Oxidized glutathione is reduced by nicotinamide adenine dinucleotide phosphate (NADP) through a reaction that is catalyzed by glutathione reductase. Glutathione reductase links the redox buffer glutathione to the anabolic redox pool of NADPH, which is mainly generated in the pentose phosphate pathway and, in the case of plants and cyanobacteria, in the light phase of photosynthesis. The major catabolic redox coenzyme is nicotinamide adenine dinucleotide (NAD) which lacks one phosphate group in comparison to NADP and thus has different binding properties, enabling enzymes to differentiate between NAD and NADP. The redox pools of NAD/NADH and NADP/NADPH are connected through the enzyme nicotine amide nucleotide transhydrogenase, a multi-domain membrane protein (Pedersen et al. 2008). Quinones, especially ubiquinone,

plastoquinone, menaquinone and related molecules play a central role in many bioenergetic reactions. Quinones take up electrons from various metabolic reactions and can channel their redox-energy into the Q-cycle that is catalyzed by *bc*-type cytochromes (Mitchell 1976; Crofts 2004). These membrane-linked redox buffers are in contact with the redox buffers in the aqueous medium in the cell through several enzymes. A description of the mechanism of *bc*-type cytochromes are discussed in articles by Xia et al. Trumpower and Hasan et al. in this volume. Although this short discussion of the different redox reactions in the cell shows only the tip of the iceberg, it underlines the prevalence and importance of complex biological redox reactions for biochemical processes. Many more different redox reactions play a central role in the metabolism and we are only at the beginning of understanding what is happening in the cells and how complex enzymes direct and use the electron flow in the cell.

There are two groups of proteins that can undergo redox changes: (i) the electron transport proteins that simply take up electrons from a protein complex and transport them further to other complexes (e.g. monomeric cytochromes, ferredoxins, flavodoxins, thioredoxins, and cupredoxins); (ii) the large group of oxido-reductase enzymes which catalyze redox reactions often with the help of metal ions or other prosthetic groups. The first group played an important role in the theoretical analysis of electron transport in proteins since they are relatively simple and therefore allow a detailed study of the electron transfer reactions. Much of our understanding of electron transfer reactions in proteins originates from studies of such small proteins such as cytochrome *c* or azurin in connection with non-natural electron transfer partners (Gray and Winkler 1996). Complex oxido-reductase enzymes are instead a challenge, since they often involve many redox-active sites and couple the redox reactions for instance to protonation

reactions or conformational changes. The theoretical understanding of these complex reactions is still in its infancy, however much of the theoretical framework developed from simple electron transfer reactions can be employed.

Although electron transfer proteins often contain cofactors, there are also a few proteinogenic amino acids that are redox-active. In particular, pairs of cysteine residues, which can form disulfide bridges, are common redox-regulated motives, for instance in thioredoxins and also in many other redox sensitive proteins (Woycechowsky and Raines 2000). Furthermore, also tyrosine and tryptophan residues are known to undergo redox state changes in proteins (Warren et al. 2012). Another amino acid that can undergo redox changes in proteins is glycine, which can form radicals (Stubbe and van der Donk 1998). These glycine radicals in conjunction with a cysteine residue can catalyze complex chemical reactions in so-called glycine radical enzymes (Stubbe and van der Donk 1998). In the resting form of the enzyme, a radical is localized at a glycine residue. Upon substrate binding, the glycy radical abstracts a hydrogen atom from an adjacent cysteine residue, which then performs the actual catalytic reaction. Another redox-active amino acid that is sometimes found in proteins is seleno-cysteine in which the thiol group is replaced by a selenol group. The  $pK_a$  value of the selenol is 5.2, much lower than that of a thiol (8.3), and its redox properties are also considerably shifted (Wessjohann et al. 2007). Besides these redox-active aminoacids, there are also protein-derived cofactors that are post-translationally formed by chemical modifications of amino acids (Davidson 2007). Examples of such groups are trihydroxyphenyl-alanine quinone, lysine tyrosylquinone, cysteine tryptophylquinone or tryptophan tryptophylquinone. Other cofactors are generated by cross-linking aminoacids such as, for instance, tyrosine and histidine in the active site of cytochrome *c* oxidase.

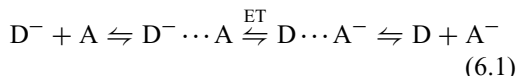
However, the large majority of electron transfer proteins bind redox cofactors as prosthetic groups. Such cofactors can be organic cofactors such as flavins or quinones; pure metal clusters such as copper centers, iron sulfur centers, non-heme iron centers, nickel-iron or molybdenum-iron centers, or manganese centers; or they can be of mixed organic/inorganic origin such as hemes or molybdopterin-centers (da Silva and Williams 2001). A special role is played by chlorophyll molecules, which are tetrapyrrole cofactors, similar to hemes, with a non-redox-active magnesium ion in the center of the ring. Pheophytins have an identical organic scaffold but lack any central ion. These later two cofactors are normally involved in light harvesting and participate in electron transfer only in photosynthetic reaction centers.

Many of the redox enzymes that perform complex reactions contain more than one redox center. Famous examples are the photosynthetic reaction center, which couples photoexcitation to charge separation, and the cytochrome  $bc_1$  and cytochrome  $b_6f$  complexes, which generate a trans-membrane proton electrochemical gradient through bifurcation reactions, and cytochrome  $c$  oxidase, which couples the exergonic reduction of oxygen to an endergonic proton transfer across the membrane. Some examples are shown in Fig. 6.1. A crucial point for the understanding of the mechanism of these enzymes is the coupling of the electron transfer reactions to proton transfer reactions, to conformational changes and to other electron transfer reactions. A theoretical analysis of electron transfer reactions can help to reveal the mechanism of complex enzymes. In order to properly model complex electron transfer reactions that are coupled to conformational changes, to proton transfer reactions, or to other chemical reactions, different theoretical methods need to be combined. In this article, we will review the most important methods and explain the theoretical framework for analyzing complex reactions.

## II. Theoretical Description of Electron Transfer Reactions

### A. Marcus Theory of Electron Transfer

Even if biological redox reactions can involve association and dissociation reactions and can thus be bimolecular (Eq. 6.1), the actual electron transfer reaction is monomolecular:



This system consists of two redox active sites, the donor (D) and the acceptor (A). In the reactant state ( $D^- \cdots A$ ), the electron is localized at the donor and in the product state ( $D \cdots A^-$ ), the electron is localized at the acceptor. The actual electron transfer step can be described by transition state theory, i.e. to obtain the following rate constants for the forward ( $k_{for}$ ) and for the backward ( $k_{back}$ ) reaction. One can write:

$$k_{for} = \frac{\zeta}{\beta h} \exp\left(-\beta G^\ddagger\right) \quad (6.2)$$

$$k_{back} = \frac{\zeta}{\beta h} \exp\left(-\beta(G^\ddagger + \Delta G^\circ)\right) \quad (6.3)$$

where  $G^\ddagger$  is the free activation energy,  $\Delta G^\circ$  is the reaction free energy,  $\zeta$  is the transmission coefficient which accounts for the probability of being reactive once the transition state is reached,  $\beta$  is  $1/k_B T$  ( $k_B$  is the Boltzmann constant,  $T$  the absolute temperature), and  $h$  the Planck constant (see Fig. 6.2).

For long range electron transfer reactions, the donor and the acceptor are only weakly electronically coupled. Thus, the reaction is non-adiabatic and its rate can be obtained from Fermi's golden rule (Marcus and Sutin 1985).

$$k_{\text{ET}} = \frac{2\pi}{h} H_{DA}^2 (FC) \quad (6.4)$$

where  $H_{DA}^2$  is the electronic coupling between the reactant state and the product state (sometimes called donor state and acceptor state, respectively) and  $(FC)$  is the

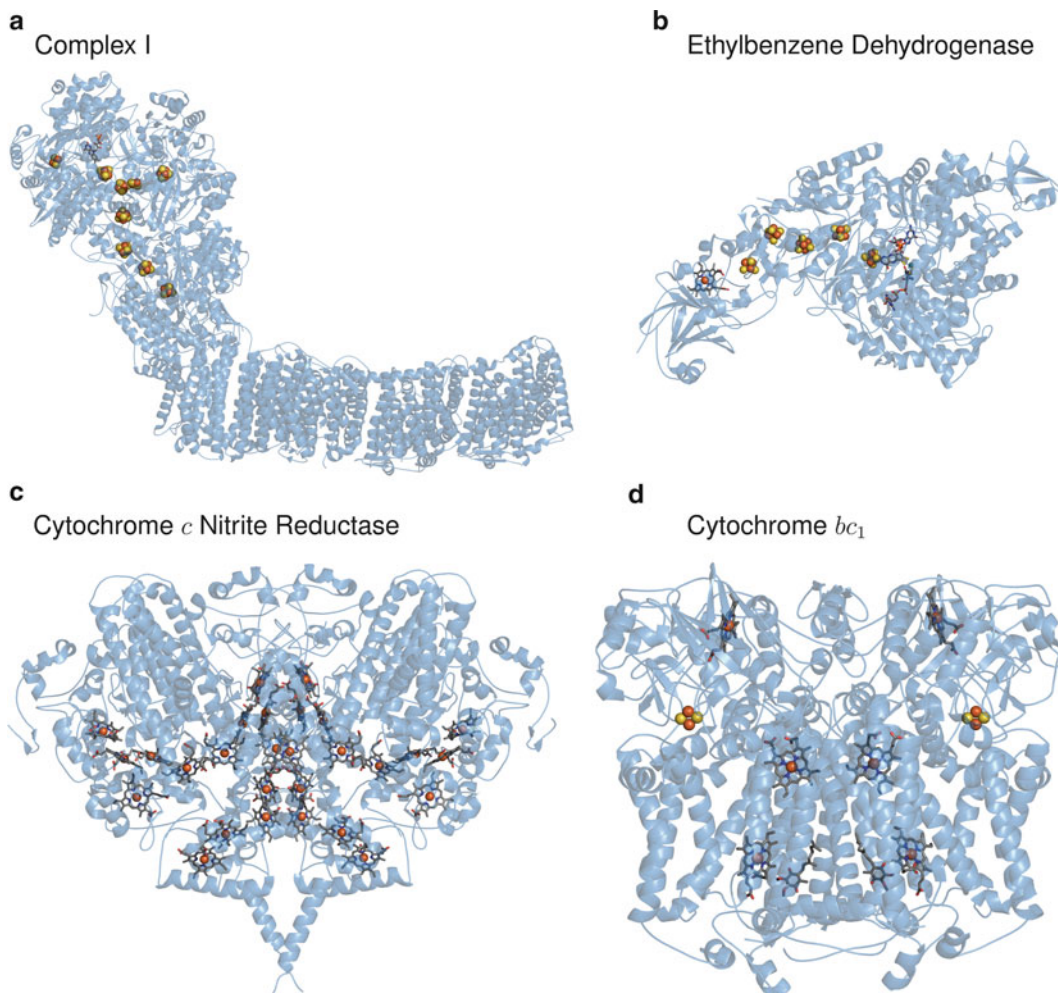


*Fig. 6.1.* Multicenter redox proteins. **(a)** Complex I catalyzes the transfer of electrons from NADH to ubiquinone. The electron transfer via several iron sulfur centers drives a proton transfer across the membrane in a not understood way. **(b)** Ethylbenzene Dehydrogenase is a molybdopterin enzyme. The electron transfer to the active site occurs via one heme and several iron-sulfur centers. **(c)** Cytochrome *c* Nitrite Reductase catalyzes the six-electron reduction of nitrite to ammonia. The electrons are provided by several heme centers in the protein. This enzyme couples the reduction of ammonia to the quinone/quinol pool in the membrane. **(d)** Cytochrome *bc*<sub>1</sub> uses the driving force of the electron transfer from ubiquinol to cytochrome *c* to generate a proton gradient. This proton pumping is achieved by a complex redox loop reaction called the Q-cycle.

Franck-Condon weighted density of states, i.e. the Franck-Condon factor. Equation 6.4 separates the electronic factors (represented by the electronic coupling) from the nuclear factors (represented by the Franck-Condon factor which accounts for the structural adaptation of the donor site, the acceptor site, and their surroundings) (Marcus and Sutin 1985). A classical form of the

Franck-Condon factor is given by the following expression:

$$(FC) = \frac{1}{\sqrt{4\pi\beta^{-1}\lambda}} \exp\left(-\beta \frac{(\Delta G^\circ + \lambda)^2}{4\lambda}\right) \quad (6.5)$$

where  $\lambda$  is the reorganization energy and  $\Delta G^\circ$  is the reaction free energy. The reor-

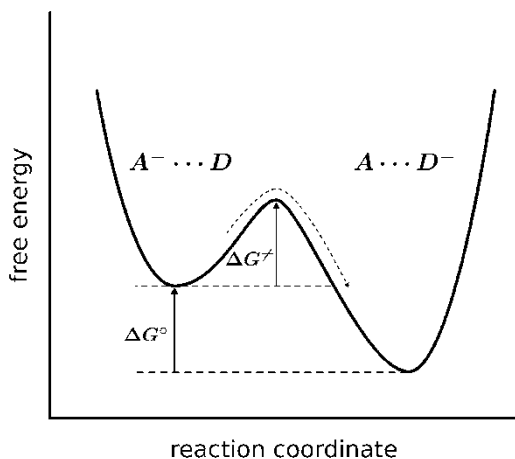


Fig. 6.2. The transition from the reactant state (or donor state) to the product state (or acceptor state) occurs over a barrier  $\Delta G^\ddagger$ . The free energy difference between the two states is  $\Delta G^\circ$ . Thus, the back reaction has a barrier that is the sum of the two energies  $\Delta G^\ddagger + \Delta G^\circ$ .

ganization energy accounts for the structural reorganization of the reactant state to the product state upon the reaction. Comparing Eq. 6.2 with Eqs. 6.4 and 6.5, one can recognize that the term  $\frac{(\Delta G^\circ + \lambda)^2}{4\lambda}$  corresponds to the activation free energy. Instead, the electronic coupling together with the preexponential factor of Eq. 6.5 are related to the transmission coefficient  $\zeta$  in Eq. 6.2.

In summary, electron transfer reactions are influenced by three energetic parameters: the electronic coupling of the donor and the acceptor, the reaction free energy, and the reorganization energy. Each of these parameters can be estimated from molecular structures using various theoretical models as discussed below.

### B. Electronic Coupling

The electronic coupling quantifies how easily an electron can move from the donor to the acceptor. The closer the donor site and the acceptor site the more rapid the transfer. If the distance between the redox centers in a protein becomes larger than 20 Å, the electron transfer rate between them is so slow

that it is basically inconsequential. The actual electron transfer is a tunneling event, in which the electronic states of the protein are used as a bridge. Several theoretical methods have been developed to calculate the tunneling efficiency.

In the simplest model, an electron with the mass  $m$  tunnels between two narrow wells that are separated by a uniform energy barrier of the height  $V$ . The electronic coupling in such a system decreases exponentially with the distance  $R$  between the wells (Gamow 1928; Gray and Winkler 2005).

$$\begin{aligned} H_{DA}^2 &= H_{DA}^\circ{}^2 \exp\left(-\frac{2\sqrt{2mV}}{\hbar}(R-R_0)\right) \\ &= H_{DA}^\circ{}^2 \exp\left(-b(R-R_0)\right) \end{aligned} \quad (6.6)$$

This model describes reasonably well the distance and the barrier height dependence of electron transfer between two cofactors embedded in a protein matrix. This picture captures the view that the electronic coupling between redox cofactors in a protein medium is mainly dependent on the distance between the cofactors. The intervening medium represents a barrier to the electron. The protein medium lowers the barrier compared to the vacuum and provides an electronic bridge. To estimate electronic coupling between cofactors in a protein, different models have been developed ranging from methods based on quantum chemical calculations (Stuchebrukhov 2003), to electron transfer pathways (Gray and Winkler 1996), or a simple, experimentally parametrized distance dependence (Moser et al. 1992; Page et al. 1999) just to name some of the models [also see Krishtalik in this volume]. In the later model, the specific nature of the intervening protein medium such as secondary or tertiary structure is not taken into consideration. Surprisingly, the different methods gave similar results leading to an exponential decay of the electronic coupling as a function of the distance between the donor site and the acceptor site. This finding indicates that the

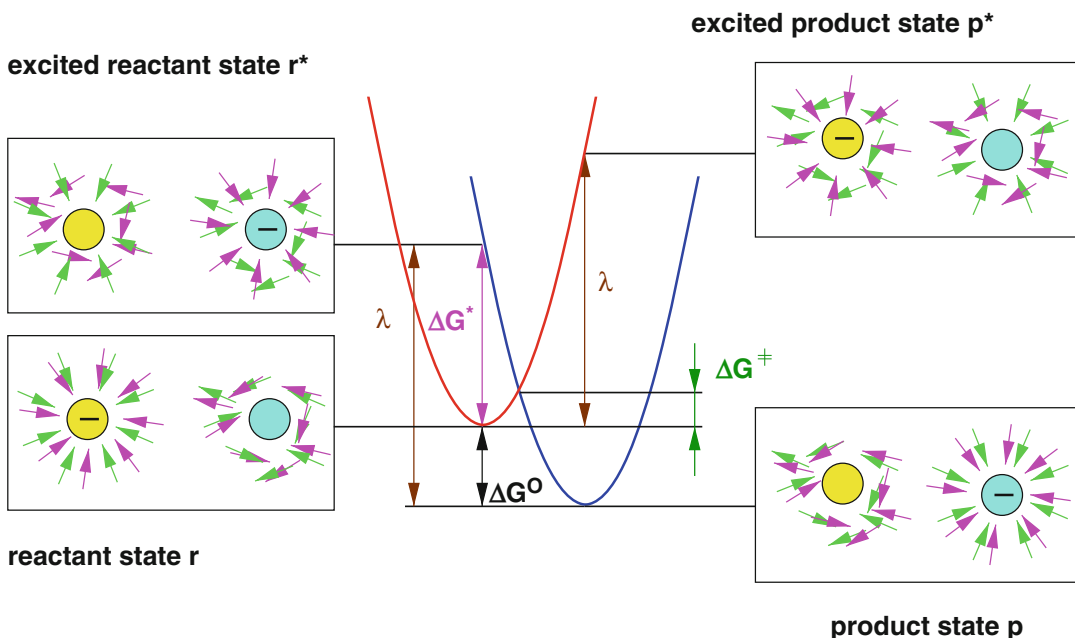


Fig. 6.3. The Marcus model of electron transfer. The reactant and the product states are described as *red* and *blue* harmonic potentials, respectively. The energy difference between the two states, i.e. the reaction free energy, is given by  $\Delta G^\circ$ . The energy  $\Delta G^*$  represents the vertical excitation energy leading to the Franck-Condon state. The reorganization energy  $\lambda$  is the energy required to adopt the nuclear configuration of the product state without leaving the potential energy curve of the reactant state. The same reorganization energy can be defined for the backward reaction. As can be seen,  $\lambda = \Delta G^\circ + \Delta G^*$ . The activation free energy  $\Delta G^\ddagger$  can be obtained from the reorganization energy and the reaction free energy. The idea of Marcus was to separate the fast relaxing electronic polarization (represented by *magenta arrows*) from the slowly relaxing solvent polarization (represented by *green arrows*). In the equilibrium states, both polarizations adapt fully to the given charge distribution, while in the vertically excited Franck-Condon state only the electronic polarization is adapted to the charge distribution.

electronic coupling is not much influenced by the specific nature of the protein medium.

### C. Reorganization Energy

The reorganization energy  $\lambda$  accounts for the structural reorganization of the reactant and the product state including the surrounding medium. Figure 6.3 shows the meaning of the reorganization energy. Assuming a harmonic potential, the reorganization energy is the energy required to adapt the geometry of the product state in the reactant state and vice versa. The potential energy of the two states can then be expressed as

$$V_r(\vec{x}) = G_r + \frac{1}{2}k(\vec{x} - \vec{x}_r)^2 \quad (6.7)$$

$$V_p(\vec{x}) = G_p + \frac{1}{2}k(\vec{x} - \vec{x}_p)^2 \quad (6.8)$$

where  $\vec{x}$  represents the collective coordinates of the system, i.e. the position of all atoms, the index  $p$  indicates the product state, the index  $r$  the reactant state, and  $k$  is a force constant. The reorganization energy is given by

$$\lambda = \frac{1}{2}k(\vec{x}_p - \vec{x}_r)^2 \quad (6.9)$$

Since the electron transfer reaction is accompanied with large changes in the electrostatic potential because of the transferred charge, the effects on the medium surrounding the redox-active sites can be rather long range (on the order of 20 Å). Therefore, it is appropriate to separate the reorganization energy into an inner sphere reorganization

energy  $\lambda_i$  and an outer sphere reorganization energy  $\lambda_o$ .

$$\lambda = \lambda_i + \lambda_o \quad (6.10)$$

The inner sphere reorganization energy is mainly connected to changes in the redox active site itself and can be calculated by an expression that is similar to Eq. 6.9. The outer reorganization energy is connected to changes in the surrounding medium such as the solvent or the protein environment. Marcus suggested that the outer sphere reorganization energy can be calculated on the basis of a continuum electrostatic model (Marcus 1956). Namely, the idea is to separate the fast electronic response ( $10^{-15} \dots 10^{-16}$  s) from the slow molecular (orientational) response ( $10^{-11} \dots 10^{-14}$  s) as explained in Fig. 6.3. This part can be described by an electrostatic model as will be discussed below (section “III.B. Calculating the Outer Sphere Reorganization Energies”).

#### D. Reaction Free Energy

The reaction free energy  $\Delta G^\circ$  is often approximated by the difference between the donor and acceptor redox groups. Even if this approximation is often justified, it is not always correct, since the interaction between the redox active groups influences the reaction free energy (Ullmann and Bombarda 2013). The situation becomes even more complex when the redox reaction is coupled to proton binding or the protein contains many redox active cofactors. Instead, it is always correct to consider the reaction free energy as the energy difference between the product state and the reactant state:

$$\Delta G = G_p - G_r \quad (6.11)$$

The microstate model (Becker et al. 2007; Bombarda and Ullmann 2011; Ullmann and Bombarda 2013), which will be explained in section “III.D. Interacting Redox Active Groups,” takes this energy difference correctly into account.

#### E. Moser-Dutton Ruler

A practical although not exclusive way of calculating electron transfer rate constants is the Moser-Dutton ruler (Moser et al. 1992; Page et al. 1999), which represents an empirical formula for electron transfer rates that relies on the theoretical basis of Marcus theory. The parameters were obtained by fitting known electron transfer rates to a linear equation of the form

$$\lg k_{et}^{ex} = A - B(R - R_o) - C \frac{(\Delta G^\circ + \lambda)^2}{\lambda} \quad (6.12)$$

$A$  was found to be 13.0;  $B$  has an average value of  $0.6 \text{ \AA}^{-1}$  (a more complex expression can be used if the packing density is considered (Page et al. 1999));  $C$  has a value of  $3.1 (\text{eV})^{-1}$ .  $R_o$  is the van der Waals contact distance, which was assumed to be  $3.6 \text{ \AA}$ . For endergonic reaction, Eq. 6.12 was extended to account for the uphill step (Eq. 6.13) with  $D = 0.06 \text{ eV}$ .

$$\lg k_{et}^{ex} = A - B(R - R_o) - C \frac{(-\Delta G^\circ + \lambda)^2}{\lambda} - \frac{\Delta G^\circ}{D} \quad (6.13)$$

The justification of Eq. 6.13 has been discussed in the literature and an alternative formulation based on the Marcus equation was proposed (Crofts and Rose 2007).

There are several other methods to estimate electron transfer rates. One of the more popular methods is the pathway model that was developed by Gray, Beratan, Onuchic, and coworkers (Gray and Winkler 1996). This model estimates the electronic coupling as a product of through-bond/through-space/through-hydrogen-bond couplings. Other methods rely on quantum chemical methods (Stuchebrukhov 2003). However, a major advantage of the Moser-Dutton ruler is its simplicity and its clear connection to molecular structures. The parameter  $R$  is the edge-to-edge distance between the cofactors involved in the electron transfer process. This distance can be estimated from



crystal structures of the relevant proteins. The other two parameters, namely the reorganization energy  $\lambda$  and the reaction free energy  $\Delta G^\circ$ , can be also estimated from the structure either by molecular mechanics calculations (Beveridge and DiCapua 1989; Muegge et al. 1997) or by continuum electrostatic calculations (Sharp 1998; Ullmann and Knapp 1999).

#### F. Tuning of Electron Transfer Rates in Proteins

The protein can tune electron transfer rate constants by adapting the three energetic parameters of the Marcus equation: the electronic coupling, the reorganization energy and the reaction free energy. As discussed above, the electronic coupling between the redox cofactors can only be efficiently varied by changing the distance between them. Changing protein residues in the electron pathways between the donor moiety and the acceptor moiety has

only minor effects presumably because the packing between the donor and the acceptor does not change very much and thus the electron always finds pathways that are equally well-suited to transfer the electron (Ullmann and Kostić 1995). Thus, in a given protein fold, the electron coupling cannot be much changed unless larger conformational changes occur. An example of such a conformational change affecting electron transfer reactions is the movement of the Rieske-head domain in cytochrome  $bc_1$  shown in Fig. 6.4 (Zhang et al. 1998).

As discussed above, another parameter of the Marcus equation is the reorganization energy. The inner sphere reorganization energy is mainly connected to the nature of the redox active group (Olsson et al. 1998; Ryde and Olsson 2001). The protein can influence this parameter only to some extent, for instance through strain exerted on the redox center. The outer sphere reorganization energy is connected to the solvent and protein reorganization. Thus, this parameter cannot also be

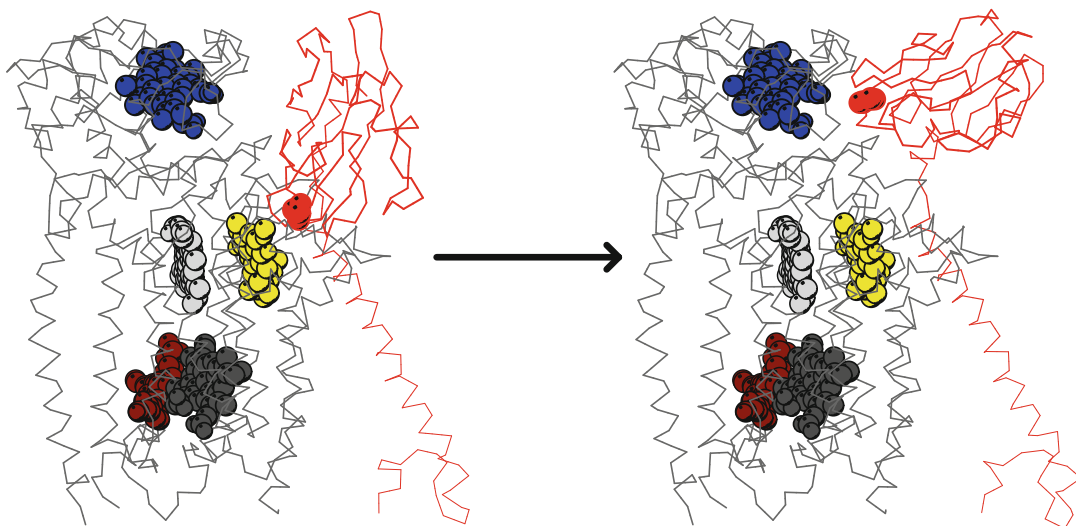


Fig. 6.4. Movement of the Rieske-Domain in cytochrome  $bc_1$ . The Rieske iron sulfur center (red balls) receives an electron from an ubiquinol (yellow) and transports this electron to cytochrome  $c_1$ . The second electron of the ubiquinol is transferred to the heme  $b_p$  (light grey) and from there further to the heme  $b_n$  (dark grey) and a quinone (brown). The subscript  $p$  or  $n$  indicate whether the heme is closer to the electrochemically positive or negative side of the membrane, respectively. The conformational change of the Rieske domain (shown in red) facilitates the electron transfer from the Rieske iron sulfur center to cytochrome  $c_1$  by changing the electronic coupling between the redox centers. The movement of the Rieske domain is a key element of the Q-cycle through which the cytochrome  $bc_1$  complex can generate a proton gradient.

much influenced in a given protein scaffold, since the protein has a low polarizability. Nevertheless, the outer sphere reorganization energy is influenced by the solvent exposure of the redox active group and the polarity of the protein medium.

The parameter that is most easily influenced by the protein environment is the reaction free energy. Biological systems have several ways to tune the redox properties of a particular site. The nature of the redox active site is the most crucial. Depending on whether an iron-sulfur cluster or a heme is chosen as a redox site, the redox potential will be different. Also the nature of the ligands of the metal center influences the redox properties. Thus, for instance it is known from model compounds of heme proteins, that the change from a histidine-histidine ligated heme to a histidine-methionine ligated heme decreases the redox potential from  $-70$  to  $-220$  mV (Wilson 1983). The protein environment is probably most important for the fine tuning of redox properties of a redox-active site (Zheng and Gunner 2009). The protein environment can tune the redox potential by (i) placement of charges or dipoles in the vicinity of the redox active site (for instance hydrogen bonds or salt bridges), (ii) changing the solvent accessibility of the redox active site, and (iii) coupling of the reduction to the protonation of a nearby site (redox-Bohr effect).

### III. Electrostatic Methods for Estimating Reaction Free Energies and Reorganization Energies

The protein can electrostatically tune the redox potential of a redox active group. This tuning can be understood theoretically by using a continuum electrostatic model of the protein.

#### A. The Poisson-Boltzmann Equation

Electrostatic interactions are the most important interactions in biomolecules. Most of the effects in biochemical systems are

dominated by electrostatics. It is therefore not too surprising that an electrostatic model can describe very well many features of biomolecular systems. This model relies on the Poisson-Boltzmann equation.

The basic idea of the Poisson-Boltzmann model is to describe the protein as a region with a low dielectric permittivity which is embedded in a region of high dielectric permittivity (aqueous solvent). The charge distribution of the protein is described by a fixed charge distribution in the low dielectric region, which is given by the molecular structure of the protein. Charges and dipoles are modeled by (fractional) point charges that are placed at the center of the atoms. The dissolved ions are represented by a Boltzmann-distributed charge density. The boundary of the low dielectric region is defined by the solvent accessible surface of the protein (Connolly 1983). Mathematically, the whole system is described by the Poisson-Boltzmann equation (Eq. 6.14) (Warwicker and Watson 1982; Honig and Nicholls 1995),

$$\begin{aligned} \nabla [\varepsilon(\mathbf{r})\nabla\phi(\mathbf{r})] = & -\rho_f(\mathbf{r}) - \sum_{i=1}^K c_i^{\text{bulk}} Z_i e_0 \\ & \times \exp\left(\frac{-Z_i e_0 \phi(\mathbf{r})}{RT}\right) \end{aligned} \quad (6.14)$$

where  $\nabla$  is the differential operator,  $\varepsilon(\mathbf{r})$  is the spatially varying dielectric permittivity,  $\rho_f(\mathbf{r})$  is the spatially fixed charge density which is usually defined by point charges at the positions of the nuclei of the solute molecule;  $c_i^{\text{bulk}}$  is the bulk concentration of the ionic species  $i$  with the charge  $Z_i$  ( $e_0$  is the elementary charge). The sum runs over all  $K$  ionic species in the solvent and describes a Boltzmann distribution of the ions in the electrostatic potential  $\phi(\mathbf{r})$  of the protein. The electrostatic potential  $\phi(\mathbf{r})$  can be obtained by solving Eq. 6.14.

Generally, non-linear partial differential equations like the one in Eq. 6.14 are difficult to solve even numerically. However by approximating the exponential term as a

series, Eq. 6.14 can be linearized. With the common definitions of the ionic strength

$$I = \frac{1}{2} \sum_{i=1}^K c_i^{\text{bulk}} Z_i^2 \quad \text{and the modified inverse}$$

Debye length  $\bar{\kappa} = \sqrt{\frac{2N_A e_0^2 I}{k_B T}}$  the linearized Poisson-Boltzmann equation assumes the form that is found in biophysics text books (Eq. 6.15).

$$\nabla [\varepsilon(\mathbf{r}) \nabla \phi(\mathbf{r})] = -\rho_{\text{prot}}(\mathbf{r}) + \bar{\kappa}^2(\mathbf{r}) \phi(\mathbf{r}) \quad (6.15)$$

In Eq. 6.15, the term  $\varepsilon(\mathbf{r})$  reflects the spatially varying permittivity (or dielectric constant). The first term on the right hand side describes the spatially fixed charge distribution in the protein and the second term describes the charge distribution due to the mobile ions which adopt a Boltzmann distribution in the field of the protein.

The Poisson-Boltzmann equation in its linearized form can be solved analytically only for particular geometries. However, there are several methods that can solve the Poisson-Boltzmann equation numerically for arbitrary geometries. The solution of the Poisson-Boltzmann equation can be expressed as a potential that is composed of two contributions:

$$\phi(\mathbf{r}) = \sum_{i=1}^M \frac{q_i}{4\pi \varepsilon_p |\mathbf{r} - \mathbf{r}'_i|} + \phi_{\text{rf}}(\mathbf{r}) \quad (6.16)$$

First, the Coulomb potential at the position  $\mathbf{r}$  caused by  $M$  point charges  $q_i$  at positions  $\mathbf{r}'_i$  in a medium with a permittivity  $\varepsilon_p$ , and second, the reaction field potential arising from the  $M$  point charges  $q_i$  and the dielectric boundary between the protein and the solvent, as well as from the distribution of ions in the solution. The reaction field potential originates from the polarization of the solvent by the solute. Usually, the reaction field potential stabilizes charged states. At the molecular level, a smaller part of this polarization originates from the deformation of the electron density of the solvent due to the presence of the solute, while the larger part originates from the orientational polarization of the solvent molecules.

The total electrostatic energy of a system in aqueous solution consists of two parts: the interaction between the components of the system and the interaction of the system with the solvent. The first contribution is obtained by charging the charge set  $\rho_2$  in the presence of the electrostatic potential caused by charge  $\rho_1$ . Assuming that the charge set  $\rho_2$  consists of a single charge  $q_f$ , the interaction energy becomes

$$G_{\text{inter}} = \int_0^{q_f} \phi(\rho_1, \mathbf{r}_q) dq = \phi(\rho_1, \mathbf{r}_q) q_f \quad (6.17)$$

Since the potential  $\phi(\rho_1, \mathbf{r}_q)$  at the position  $\mathbf{r}_q$  of the charge  $q_f$  is totally independent of the charge  $q_f$  itself, the integration in Eq. 6.17 reduces to a simple multiplication. Equation 6.17 can be generalized to the interaction between two disjunct sets of charges  $\{q\}$  and  $\{p\}$ , which is given by

$$G_{\text{inter}} = \sum_{i=1}^{N_q} q_i \phi(\{p\}, \mathbf{r}_{q_i}) = \sum_{i=1}^{N_p} p_i \phi(\{q\}, \mathbf{r}_{p_i}) \quad (6.18)$$

where  $N_q$  and  $N_p$  are the number of charges in the charge sets  $\{q\}$  and  $\{p\}$ , respectively,  $\phi(\{p\}, \mathbf{r}_{q_i})$  is the potential caused by the charge set  $\{p\}$  at the position of the charge  $q_i$  and  $\phi(\{q\}, \mathbf{r}_{p_i})$  is the potential caused by the charge set  $\{q\}$  at the position of the charge  $p_i$ . As can be seen from Eq. 6.18, this interaction energy is symmetric.

The second contribution is the reaction field energy, which is also sometimes called “self-energy”. This energy originates from the interaction energy of the charge set  $\{q\}$  with its own reaction field potential  $\phi_{\text{rf}}$ . To obtain this energy, one imagines the charging of a particle in a dielectric medium, and asks what is the energy of this charging process. Analogous to Eq. 6.17, we can write

$$G_{\text{rf}} = \int_0^{q_f} \phi_{\text{rf}}(q, \mathbf{r}_q) dq \quad (6.19)$$

In contrast to the situation in Eq. 6.17, the reaction field potential  $\phi_{\text{rf}}$  depends on the

charge of the particle. For simplicity, one assumes a linear response, i.e.  $\phi_{rf}(q_f, \mathbf{r}_q) = Cq_f$ . From Eq. 6.19, we obtain

$$G_{rf} = \int_0^{q_f} Cq \, dq = \frac{1}{2} Cq_f^2 = \frac{1}{2} \phi_{rf}(q_f, \mathbf{r}_q) q_f \quad (6.20)$$

Equation 6.20 can be generalized to obtain the reaction field energy of a charge set  $\{q\}$

$$G_{rf} = \frac{1}{2} \sum_{i=1}^{N_q} q_i \phi_{rf}(\{q\}, \mathbf{r}_{q_i}) \quad (6.21)$$

As shown above, the factor  $\frac{1}{2}$  in this equation is a consequence of the linear response approach.

The reaction field energy can be used to calculate the electrostatic contribution of the solvation energy, which is the energy to transfer from vacuum into a solvent with a given dielectric constant  $\epsilon_s$ . This approach was used by Max Born to calculate the solvation energy of an ion with the radius  $r$  and the charge  $Z$  (Born 1920)

$$\Delta G_{solv} = -\frac{1}{4\pi\epsilon_o} \frac{(Ze_o)^2}{2r} \left(1 - \frac{1}{\epsilon_s}\right) \quad (6.22)$$

This equation is part of an expression for the outer reorganization energy derived by Marcus (1956), which will be discussed in the next section.

Although the continuum electrostatic approach is relatively simple, it is surprising how well it works to understand the energetics of biochemical systems (Ullmann et al. 2008). It can be used to analyze electron and proton transfer reactions as will be explained in the following.

### B. Calculating the Outer Sphere Reorganization Energies

By separating the fast and the slow polarization, Marcus derived a simple expression for the outer sphere reorganization energy for the transfer of the charge  $\Delta e$  between two spherical ions with the radii  $a_1$  and  $a_2$

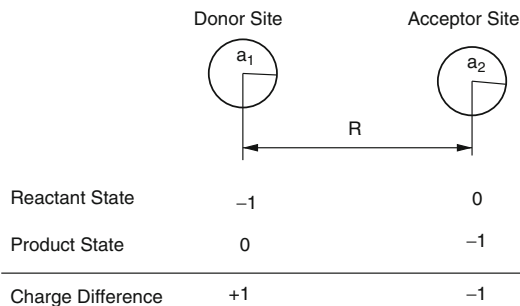


Fig. 6.5. Model of the charge transfer between two spheres at a separation  $R$  with the radii  $a_1$  and  $a_2$ , respectively. The charge difference between the product state and the reactant state can be used to calculate the outer sphere reorganization energy and leads to Eq. 6.23.

at a distance  $R$  (Marcus 1956), leading to Eq. 6.23

$$\lambda_o = \frac{\Delta e^2}{4\pi\epsilon_o} \left( \frac{1}{2} \left( \frac{1}{a_1} + \frac{1}{a_2} \right) - \frac{1}{R} \right) \left( \frac{1}{\epsilon_{op}} - \frac{1}{\epsilon_s} \right) \quad (6.23)$$

where  $\epsilon_{op}$  is the optical dielectric constant and  $\epsilon_s$  is the dielectric constant of the solvent (Fig. 6.5). The optical dielectric constant takes into account only the electronic polarization and thus has a value of about 2.

Equation 6.23 can be interpreted as having two contributions: (i) the difference between the solvation energy of ions in a low dielectric medium with a purely electronic polarization ( $\epsilon_{op}$ ) and a solvent with a higher dielectric constant  $\epsilon_s$  and (ii) interaction energy of the charge difference between the reactant and the product state. Since the charge difference is considered, the charge at the donor site and the acceptor site is  $+1$  and  $-1$ , respectively. The interaction between these charges gives rise to the  $1/R$  term. The solvation energy difference is related to the Born formula (Eq. 6.22). Thus, the influence of the reaction field originating from the donor site is neglected at the acceptor site and vice versa. This approximation is valid if  $R$  is large. The outer sphere reorganization energy is always a positive number, since the optical dielectric constant, which

accounts only for the purely electronic polarization, is much smaller than the solvent dielectric constant and the separation between the charges is much larger than the radius of the spheres.

The idea that underlies Eq. 6.23 can be generalized such that it can be used to calculate the reorganization energy of a protein (Sharp 1998). For proteins, the numerical solution of the Poisson-Boltzmann equation must be used instead of the Born formula. The outer sphere reorganization energy in this frame work is given by

$$\lambda_o = \frac{1}{2} \sum_i \left( \phi_{r^*-r}(\{\Delta q\}, \mathbf{r}_i) - \phi_{p-r}(\{\Delta q\}, \mathbf{r}_i) \right) \Delta q_i \quad (6.24)$$

where the charge set  $\{\Delta q\}$  is the difference between charges assigned to the product state and the reactant state, respectively

$$\Delta q_i = q_i^p - q_i^r \quad (6.25)$$

In Eq. 6.24, the term  $\phi_{r^*-r}(\{\Delta q\}, \mathbf{r}_i)$  reflects the potential considering the fast electronic relaxation and is the numerical solution of Eq. 6.26

$$\nabla \varepsilon_{op} \nabla \phi_{r^*-r}(\{\Delta q\}) = -\rho(\{\Delta q\}) \quad (6.26)$$

The term  $\phi_{p-r}(\{\Delta q\}, \mathbf{r}_i)$  represents the potential considering slow orientational relaxation which is given by the numerical solution of Eq. 6.27

$$\nabla \varepsilon(\mathbf{r}) \nabla \phi_{p-r}(\{\Delta q\}) = -\rho(\{\Delta q\}) + \bar{\kappa}^2 \phi_{p-r}(\{\Delta q\}) \quad (6.27)$$

With this approach, the reorganization energy of a charge transfer reaction can be easily calculated on the basis of molecular structures using the numerical solution of the Poisson-Boltzmann equation. Interestingly, in this approach the outer sphere reorganization energy depends only on the charge difference between the reactant state and the donor state and to a minor extent on the shape of the low dielectric region defined by the protein. Thus, in the frame

work of this continuum electrostatic model, the surrounding protein residues do not have much influence on the outer sphere reorganization energy except by defining the dielectric boundaries. Consequently, one would expect that the reorganization energy cannot be much altered by mutations.

### C. Calculating Redox Potentials of Proteins

The redox potential of a group characterizes the energetics of an electron transfer reaction, since it is proportional to the energy change upon electron release or uptake. The calculation of absolute redox potentials requires very high-level quantum chemical calculations and is often not very accurate. However, changes in the redox potentials arising from the protein are mainly caused by electrostatic interactions. Thus, it is possible to determine the changes of the redox potential of a group  $A$  due to the protein environment compared to a model compound of the group for which the redox potential  $E_{\text{model},A}^o$  is known. There are two contributions to the redox potential shift, one originates from the changes of the reaction field when the model compound is moved from the aqueous solution into the protein ( $\Delta \Delta G_{\text{Born},A}^{\text{redox}}$ ). The other originates from the interaction of the redox active group with the charges and dipoles of the protein ( $\Delta \Delta G_{\text{back},A}^{\text{redox}}$ ). The redox potential in the protein  $E_{\text{intr},A}^o$  is thus expressed by

$$E_{\text{intr},A}^o = E_{\text{model},A}^o - \frac{1}{F} (\Delta \Delta G_{\text{Born},A}^{\text{redox}} + \Delta \Delta G_{\text{back},A}^{\text{redox}}) \quad (6.28)$$

where

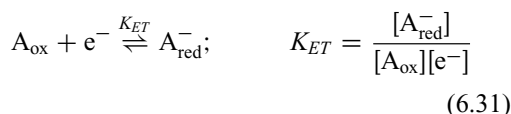
$$\begin{aligned} \Delta \Delta G_{\text{Born},A}^{\text{redox}} &= \frac{1}{2} \sum_{i=1}^{N_{Q,A}} Q_{i,A}^{\text{red}} [\phi_p(\mathbf{r}_i; Q_A^{\text{red}}) - \phi_m(\mathbf{r}_i; Q_A^{\text{red}})] \\ &\quad - \frac{1}{2} \sum_{i=1}^{N_{Q,A}} Q_{i,A}^{\text{ox}} [\phi_p(\mathbf{r}_i; Q_A^{\text{ox}}) - \phi_m(\mathbf{r}_i; Q_A^{\text{ox}})] \end{aligned} \quad (6.29)$$

$$\begin{aligned}
\Delta\Delta G_{\text{back},A}^{\text{redox}} &= \sum_{i=1}^{N_p} q_i [\phi_p(\mathbf{r}_i; Q_A^{\text{red}}) - \phi_p(\mathbf{r}_i; Q_A^{\text{ox}})] \\
&\quad - \sum_{i=1}^{N_m} q_i [\phi_m(\mathbf{r}_i; Q_A^{\text{red}}) - \phi_m(\mathbf{r}_i; Q_A^{\text{ox}})]
\end{aligned} \tag{6.30}$$

The summations in Eq. 6.29 run over the  $N_{Q,A}$  atoms of group  $A$  that have different charges  $Q_{i,A}^{\text{ox}}$  and  $Q_{i,A}^{\text{red}}$  in the oxidized (ox) and in the reduced (red) state, respectively. The first summation in Eq. 6.30 runs over the  $N_p$  charges of the protein that belong to atoms in non-titratable groups. The second summation in Eq. 6.30 runs over the  $N_m$  charges of atoms of the model compound that do not have different charges in the different redox states. The terms  $\phi_m(\mathbf{r}_i, Q_A^{\text{ox}})$ ,  $\phi_m(\mathbf{r}_i, Q_A^{\text{red}})$ ,  $\phi_p(\mathbf{r}_i, Q_A^{\text{ox}})$ , and  $\phi_p(\mathbf{r}_i, Q_A^{\text{red}})$  denote the values of the electrostatic potential at the position  $\mathbf{r}$  of the atom  $i$ . The electrostatic potential can be obtained by solving the Poisson-Boltzmann equation numerically using the shape of either the protein (subscript  $p$ ) or the model compound (subscript  $m$ ) as dielectric boundary and assigning the charges of the redox-active group  $A$  in either the oxidized ( $Q_A^{\text{ox}}$ ) or the reduced ( $Q_A^{\text{red}}$ ) form to the respective atoms.

The background energy  $\Delta\Delta G_{\text{back},A}^{\text{redox}}$  reflects the interaction of the redox-active group with charges of the protein. Thus, it is this term that is mainly influenced by mutations of residues or by variations of the protonation state of nearby residues. The Born term  $\Delta\Delta G_{\text{Born},A}^{\text{redox}}$  is sensitive to changes in the protein shape and thus it may change in case the border between protein and solvent is modified by mutations or by conformational changes in the vicinity of the active site.

The equilibrium between the redox couple  $A_{\text{ox}}/A_{\text{red}}^-$  is defined by



where  $K_{ET}$  is the equilibrium constant. One can define the solution redox potential  $E$  and the redox potential  $E^0$  of the redox couple  $A_{\text{ox}}/A_{\text{red}}^-$  as  $E = -RT/F \ln \gamma[e^-]$  and  $E^0 = RT/F \ln K_{ET}$ , respectively. With the factor  $RT/F$ , where  $F$  is the Faraday constant, one obtains  $E$  and  $E^0$  in the units volts;  $\gamma$  is the activity coefficient. The relation between  $E^0$  and the standard reaction free energy  $G_{\text{redox}}^0$  is given by  $G_{\text{redox}}^0 = FE^0$ . With these definitions and Eq. 6.31, one obtains the Nernst equation for a single electron reduction:

$$E = E^0 + \frac{RT}{F} \ln \frac{[A_{\text{ox}}]}{[A_{\text{red}}^-]} \tag{6.32}$$

The probability  $\langle x \rangle$  that a redox-active group is in its oxidized state is defined as  $\langle x \rangle = [A_{\text{ox}}]/([A_{\text{red}}^-] + [A_{\text{ox}}])$ . The relation between the probability  $\langle x \rangle$ , the solution redox potential  $E$ , and the redox potential  $E^0$  is given by

$$\langle x \rangle = \frac{\exp\left(\frac{F}{RT}(E - E^0)\right)}{1 + \exp\left(\frac{F}{RT}(E - E^0)\right)} \tag{6.33}$$

Consequently, the free energy  $G_{\text{redox}}$  required to oxidize a one-electron redox-active group at a given redox potential of the solution  $E$  is given by Eq. 6.34.

$$G_{\text{redox}} = -F(E - E^0) = -RT \ln \frac{\langle x \rangle}{1 - \langle x \rangle} \tag{6.34}$$

#### D. Interacting Redox Active Groups

In many redox proteins, there is more than one redox active group and these redox active groups interact. Because of these interactions, the titration curves of the individual redox active sites can become irregular. These irregular titration curves originate from the population of several microstates. The simplest case is a system with two interacting sites.

Such a system has four possible microstates: fully reduced, reduced at one group, reduced at the other group, and fully oxidized (Fig. 6.6). These states can be respectively described by their redox

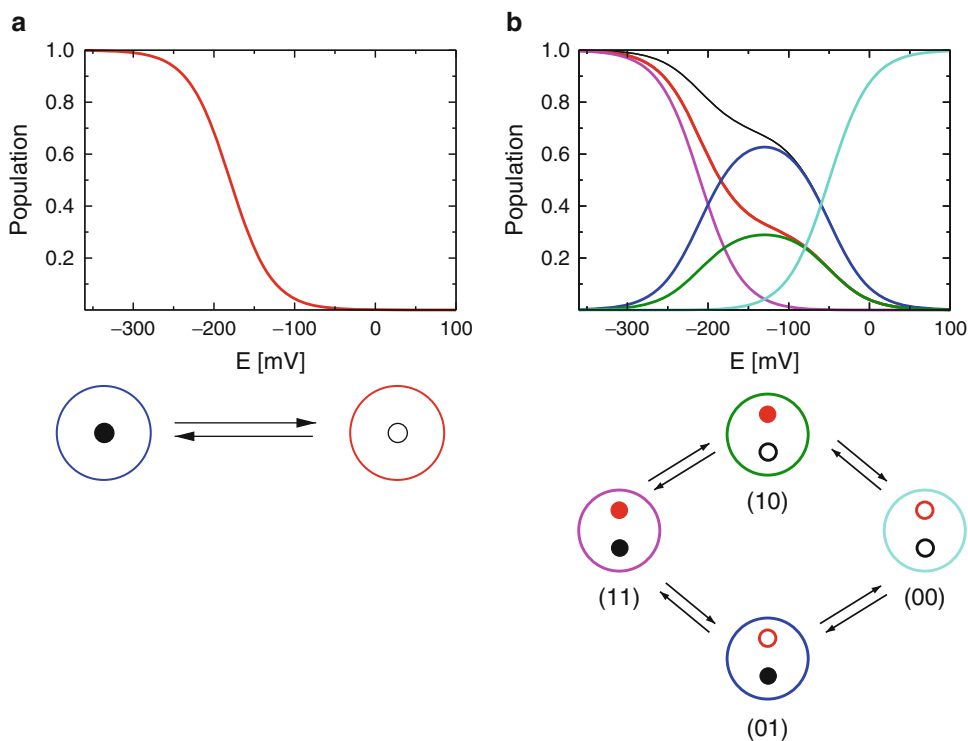


Fig. 6.6. Titration behavior of molecules with one and two redox-active groups. (a) Titration curve of a single redox-active group. The titration curve has a sigmoidal shape. (b) Titration curve of a molecule with two titratable groups. The contributions of the populations of the different microstates lead to non-sigmoidal titration curves. The microstates and their populations, the titration curves and the sites are color coded in the reaction scheme and in the diagram. For instance, the titration curve of the *red* site is the sum of the probability of the microstate population curve of the state (11) in *magenta* and the microstate population curve of state (10) in *green*.

state vectors: 11, 10, 01, and 00, where 1 marks that the group is reduced and 0 that it is oxidized. In order to obtain the titration curve of group one, the probabilities of all microstates in which this group is reduced need to be added. For instance the titration curve of group one is given by  $\langle x_1 \rangle = \langle 10 \rangle + \langle 11 \rangle$ . The titration curves of such groups can considerably deviate from standard sigmoidal titration curves and can show highly irregular features because of electrostatic interactions between the groups. The assignment of an  $E^\circ$  value to one particular group is in such cases difficult if not impossible. To eliminate the difficulties, the problem can be reformulated. Instead of considering a protein as a system of groups with a certain probability of being reduced, the problem can be formulated in terms of

well-defined microstates of the protein which have a certain probability of occurrence as will now be outlined.

Let us consider a system that possesses  $K$  redox-active sites. Such a system can adopt  $M = 2^K$  states assuming that each sites can exist in two forms. The interaction between them can be modeled electrostatically. Each state of the system can be written as a  $K$ -dimensional vector  $\vec{x} = (x_1, \dots, x_K)$ , where  $x_i$  is 1 or 0 if site  $i$  is reduced or oxidized, respectively. Each state of the system has a well-defined energy which depends on the redox energetics of the individual sites ( $E_i^{\text{intr}}$ ) and the interaction between sites ( $W_{ij}$ ). The energy of a state  $\vec{x}_v$  is given by (Bashford and Karplus 1990; Ullmann and Knapp 1999; Ullmann 2000; Gunner et al. 2006; Nielsen and McCammon 2003):

$$G(\vec{x}_v) = \sum_{i=1}^K (x_{v,i} - x_i^\circ) F(E - E_i^{\text{intr}}) + \frac{1}{2} \sum_{i=1}^K \sum_{j=1}^K (x_{v,i} - x_i^\circ)(x_{v,j} - x_j^\circ) W_{ij} \quad (6.35)$$

where  $R$  is the gas constant,  $T$  the absolute temperature, and  $F$  the Faraday constant;  $x_{v,i}$  denotes the redox form of the site  $i$  in state  $\vec{x}_v$ ,  $x_i^\circ$  is the reference form of site  $i$ ;  $E_i^{\text{intr}}$  is the redox potential that site  $i$  would have if all other sites are in their reference state (this value is also called the intrinsic redox potential; see section “III.C. Calculating Redox Potentials of Proteins”);  $E$  is the reduction potential of the solution;  $W_{ij}$  represents the interaction energy between site  $i$  and  $j$ . It can be calculated from Eq. 6.36.

$$W_{ij} = \sum_{A=1}^{N_{Q,A}} [Q_{i,A}^{\text{red}} - Q_{i,A}^{\text{ox}}] [\phi_p(\mathbf{r}_A, Q_j^{\text{red}}) - \phi_p(\mathbf{r}_A, Q_j^{\text{ox}})] \quad (6.36)$$

Equation 6.35 can be used to calculate either microscopic redox potentials or also microscopic reaction free energies by subtracting the appropriate microstate energies from each other. For example, if we consider a system with two sites as depicted in Fig. 6.6, we can calculate a microscopic redox potential from the energy difference between the states (1,0) and (1,1). This microscopic redox potential will differ from the microscopic redox potential between the states (0,0) and (0,1) because of electrostatic interactions between the two groups. The reaction free energy is given by the energy difference between the states (0,1) and (1,0). This reaction free energy can be used in Marcus theory to calculate electron transfer rates.

The equilibrium properties of a physical system are completely determined by the energies of its states. To keep the notation concise, states will be numbered by Greek indices in the subscript, i.e., for state energies we write  $G_\nu$  instead of  $G(\vec{x}_\nu)$ . For site indices, the roman letters  $i$  and  $j$  will be used.

The equilibrium probability of a single state  $\vec{x}_\nu$  is given by

$$p_\nu^{\text{eq}} = \frac{e^{-\beta G_\nu}}{Z} \quad (6.37)$$

with  $\beta = 1/RT$  and  $Z$  being the partition function of the system.

$$Z = \sum_{\nu=1}^M e^{-\beta G_\nu} \quad (6.38)$$

The sum runs over all  $M$  possible states. Properties of single sites can be obtained from Eq. 6.37 by summing up the individual contributions of all states. For example, the probability of site  $i$  being reduced is given by

$$\langle x_i \rangle = \sum_{\nu} x_{\nu,i} p_\nu^{\text{eq}} \quad (6.39)$$

where  $x_{\nu,i}$  denotes the redox form of site  $i$  in the charge state  $\vec{x}_\nu$ . For small systems, this sum can be evaluated explicitly. For larger systems, Monte-Carlo techniques can be used to determine these probabilities (Beroza et al. 1991; Ullmann and Ullmann 2012).

In general, the titration curves in such a system do not have to be sigmoidal and can even be non-monotonic (Onufriev et al. 2001). However as a consequence of statistical thermodynamics, it can be proven that the macroscopic titration curve of a system can be always decomposed into standard titration curves (Nernst functions) as long as there is no positive cooperativity (Ullmann 2003; Ullmann and Bombarda 2013).

In principle,  $2^{K-1}$  different microscopic redox potentials can be assigned to each redox-active group in a protein, where  $K$  is the number of redox active groups in the molecule. Since however, most of the interactions are relatively weak, most of these microscopic redox potentials will be very similar. But in case of strong interactions, a larger variation of the redox potential can be observed. As an example, Fig. 6.7 shows the calculated redox potentials of the hemes



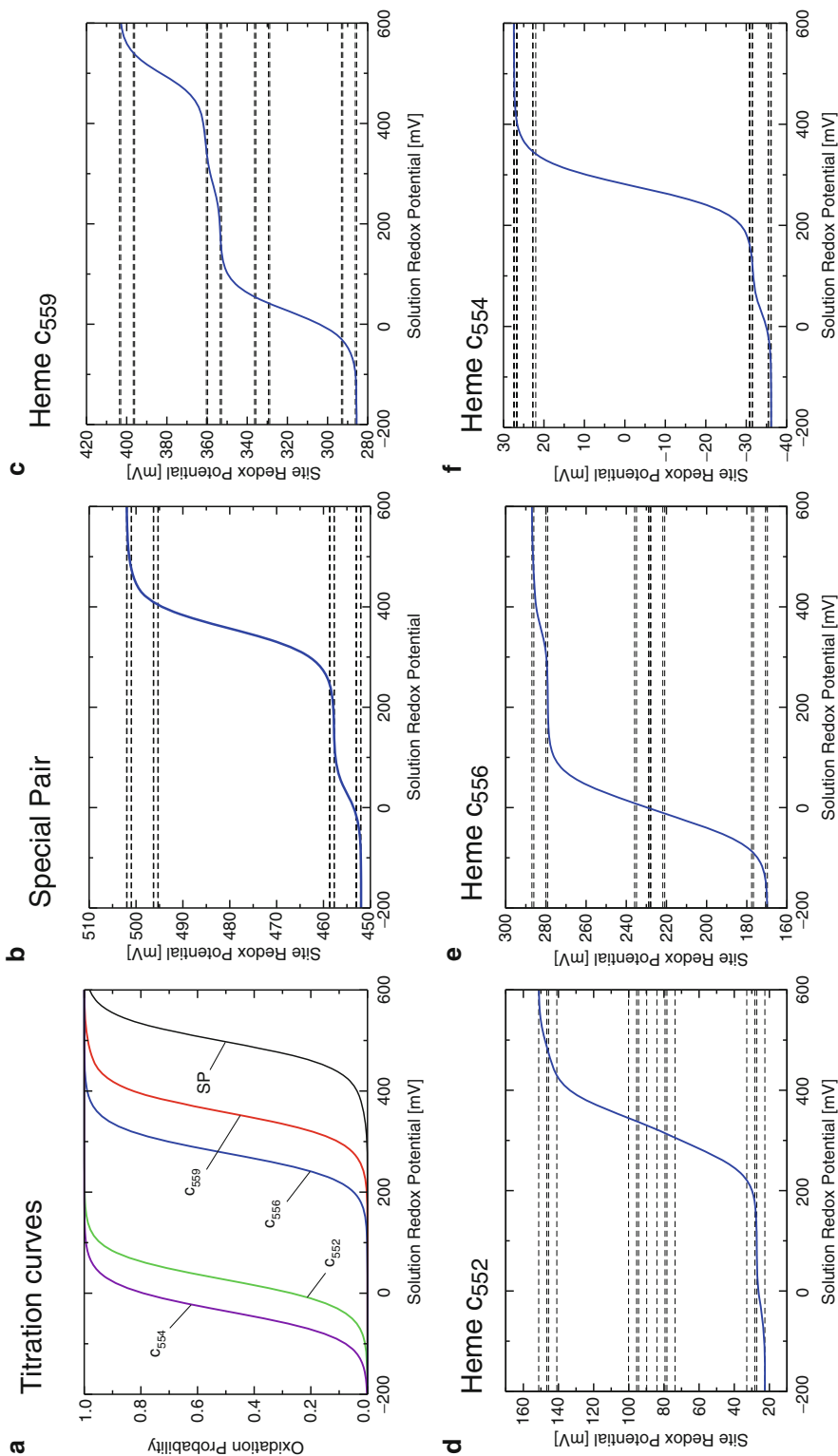


Fig. 6.7. Calculated redox titration behavior of special pair (SP) and the hemes of the RC from *B. viridis*. (a) Probability of the oxidized form of the redox-active sites; (b) to (f) solution redox-potential dependence of the site redox potential of the special pair (b), heme  $c_{559}$  (c), heme  $c_{552}$  (d), heme  $c_{556}$  (e), heme  $c_{554}$  (f). The *dashed lines* show the different microscopic redox potentials, the *blue lines* show the average redox-potential which depends on the solution redox potential.

and the special pair of bacteriochlorophylls in the photosynthetic reaction center from *B. viridis*. This protein possesses four heme groups that facilitate the rereduction of the special pair after photooxidation (Fig. 6.10). As can be seen from the graphs in Fig. 6.7, the microscopic redox potentials may vary quite substantially and cannot necessarily be read as midpoint potentials directly from the titration curves which are depicted in Fig. 6.7a. An effective redox potential or midpoint potential can be defined from the redox potential-dependent reduction probability

$$E_i^{\circ} = E - \frac{RT}{F} \left( \ln \frac{\langle x_i \rangle}{1 - \langle x_i \rangle} \right) \quad (6.40)$$

This effective midpoint potential can depend on the solution redox potential because of the interaction between the redox active sites. It represents an equilibrium redox potential (Ullmann and Bombarda 2013). The value of this effective midpoint potential varies between the most extreme microscopic redox potentials (see Fig. 6.7). However, it must be underlined that this effective midpoint potential is not necessarily the functionally relevant redox potential at which an enzyme is working as will be shown later (section “IV. Complex Electron Transfer Proteins”).

#### E. Looking at the Coupling of Reduction Reactions to Protonation Reaction

Redox reactions are often coupled to protonation reactions. Such a coupling can be very strong, meaning that as soon as an electron binds a proton also binds stoichiometrically. In other cases, the coupling is relatively weak, meaning that the coupling is substoichiometric. Biologically, this coupling of protonation and reduction can help on the one hand to tune the redox potential of a redox active group; on the other hand, it is essential for the electron transfer driven proton transfer that plays a central role in biological energy transduction (Nicholls and Ferguson 2013).

Since protonation and redox reactions can be considered in general as binding reactions, they are basically all described by the same underlying theory. Figure 6.8 summarizes and compares the similarity among the description of protonation reactions by the Henderson-Hasselbalch equation, redox equilibria by the Nernst equation, and a general thermodynamic description of binding equilibria. Because of this resemblance, protonation equilibria can be described by the same theoretical tools as redox equilibria. Since there are usually several protonatable groups in a protein, one has to consider the interaction between the protonatable groups and the mutual interaction between the protonatable groups and the redox active groups. The state vector defined above needs to be extended to a  $2^{N+K}$  dimensional vector where  $N$  is the number of protonatable groups and  $K$  is number of redox active groups. Equation 6.35 needs to be extended to include the effect of the pH.

$$\begin{aligned} G(\vec{x}_v) = & \sum_{i=1}^N (x_{v,i} - x_i^{\circ}) RT \ln 10 (\text{pH} - \text{p}K_{a,i}^{\text{intr}}) \\ & + \sum_{i=1}^K (x_{v,i} - x_i^{\circ}) F (E - E_i^{\text{intr}}) \\ & + \frac{1}{2} \sum_{i=1}^{N+K} \sum_{j=1}^{N+K} (x_{v,i} - x_i^{\circ})(x_{v,j} - x_j^{\circ}) W_{ij} \quad (6.41) \end{aligned}$$

In this equation,  $\text{p}K_{a,i}^{\text{intr}}$  is the intrinsic  $\text{p}K_a$  value, i.e., the  $\text{p}K_a$  value that the site would have if all other titratable groups are in their respective reference state. By analogy to the intrinsic redox potential, the intrinsic  $\text{p}K_a$  value is calculated using an appropriate model compound and takes into account the protonation energy shift due to the change in the solvation energy ( $\Delta\Delta G_i^{\text{Borm}}$ ) and the change due to the interaction with non-titrating background charges ( $\Delta\Delta G_i^{\text{back}}$ ).

$$\begin{aligned} \text{p}K_{a,i}^{\text{intr}} = & \text{p}K_a^{\text{model}} - \frac{1}{RT \ln 10} (\Delta\Delta G_i^{\text{Borm}} \\ & + \Delta\Delta G_i^{\text{back}}) \quad (6.42) \end{aligned}$$

Protonation	Reduction	General Binding
$\text{HA} \xrightleftharpoons{K_a} \text{A}^- + \text{H}^+$	$\text{A}_{\text{ox}} + \text{e}^- \xrightleftharpoons{K_{\text{ET}}} \text{A}_{\text{red}}^-$	$\text{R} + \text{L} \xrightleftharpoons{K} \text{RL}$
Henderson-Hasselbalch Equation	Nernst Equation	Binding Equilibrium
$\text{p}K_a = \text{pH} - \lg \frac{[\text{A}^-]}{[\text{HA}]}$	$E^\circ = E + \frac{1}{\beta F} \ln \frac{[\text{A}_{\text{red}}^-]}{[\text{A}_{\text{ox}}]}$	$G^\circ = \mu_L + \frac{1}{\beta} \ln \left( \frac{[\text{R}]}{[\text{RL}]} \right)$
pH Value	Solution Redox Potential	Chemical Potential
$\text{pH} = -\lg \left( \gamma [\text{H}^+] \right)$	$E = -\ln \left( \gamma [\text{e}^-] \right)$	$\mu_L = \mu_L^\circ + \ln \left( \gamma [\text{L}] \right)$
Protonation Energy at a given pH value	Reduction Energy at a given solution redox potential	Binding Energy at a given chemical potential
$G^{\text{prot}} = -\beta^{-1} \ln 10 (\text{p}K_a - \text{pH})$	$G^{\text{red}} = -F(E^\circ - E)$	$G^{\text{bind}} = -(G^\circ - \mu_L)$
Protonation Probability	Reduction Probability	Binding Probability
$\langle x \rangle = \frac{e^{-\ln 10 (\text{pH} - \text{p}K_a)}}{1 + e^{-\ln 10 (\text{pH} - \text{p}K_a)}}$	$\langle x \rangle = \frac{e^{-\beta F (E - E^\circ)}}{1 + e^{-\beta F (E - E^\circ)}}$	$\langle x \rangle = \frac{e^{-\beta (G^\circ - \mu_L)}}{1 + e^{-\beta (G^\circ - \mu_L)}}$

Fig. 6.8. Comparison of the theoretical formulations of protonation equilibria, redox equilibria and general binding equilibria. The direct comparison shows the equivalence of the formulations and the relationship between the corresponding terms. Moreover, it allows to see the relation protonation reactions and reduction reactions to a more general binding formalism. The meaning of the symbols is explained in the text.

These energy shifts as well as the interaction energy  $W_{ij}$  between two groups can be calculated on the basis of the Poisson-Boltzmann equation as described above (Bashford and Karplus 1990; Ullmann and Knapp 1999).

The formalism described here is applicable only to sites that have two states, i.e., either protonated and deprotonated or oxidized and reduced. For some redox active sites such as quinones or flavins, the situation is more complicated, because they have multiple redox and protonation states for just one site. Furthermore, changes in the conformation of the amino acids side chain (rotamers) as well as larger conformational changes may

need to be considered. For all such cases, the formalism needs to be extended (Ullmann and Ullmann 2012). The equations become slightly more complicated; nevertheless, the basic philosophy stays the same and the microstate model can be applied.

#### F. Influence of Membrane Potential and Transmembrane Gradients

Many electron transfer proteins are embedded in membranes and generate an electrochemical gradient consisting of a proton gradient and a membrane potential across these membranes. This electrochemical

transmembrane gradient is used by ATP-synthase membrane protein complex to transduce the electrochemical energy into chemical energy in the form of ATP. Thus, the effect of transmembrane gradients and membrane potentials also need to be considered to describe energy transduction processes properly.

The influence of a membrane potential on the energetics of a membrane protein can be incorporated in the Poisson-Boltzmann theory (Roux 1997). The linearized Poisson-Boltzmann equation (see section “III.A. The Poisson-Boltzmann Equation”) of a membrane system with a membrane potential  $\Psi$  present is given by

$$\begin{aligned} \nabla [\varepsilon(\mathbf{r})\nabla\phi(\mathbf{r})] &= -\rho_f(\mathbf{r}) + \varepsilon(\mathbf{r})\bar{\kappa}(\mathbf{r})^2 [\phi(\mathbf{r}) \\ &\quad - \Psi\Theta(\mathbf{r})] \end{aligned} \quad (6.43)$$

where  $\Theta(\mathbf{r})$  is a simple step function which is equal to zero at the extracellular side and equal to one at the cytoplasmic side (Heaviside step function). The potential  $\phi(\mathbf{r})$  which is obtained as the numerical solution of Eq. 6.43 can be expressed as (You and Bashford 1995; Roux 1997)

$$\phi(\mathbf{r}) = \sum_{i=1}^M \frac{q_i}{\varepsilon_p |\mathbf{r} - \mathbf{r}'_i|} + \phi_{\text{rf}}(\mathbf{r}) + \Psi\chi_{\text{mp}}(\mathbf{r}) \quad (6.44)$$

As in Eq. 6.16, the first term describes the Coulomb electrostatic potential at the position  $\mathbf{r}$  caused by  $M$  point charges  $q_i$  at positions  $\mathbf{r}'_i$  in a medium with a dielectric permittivity  $\varepsilon_p$ . The second term describes the reaction field potential  $\phi_{\text{rf}}(\mathbf{r})$  originating from the dielectric boundary between the protein and the solvent as well as from the distribution of ions in the solution, and the third term describes the potential originating from the transmembrane potential. In Eq. 6.44,  $\chi_{\text{mp}}(\mathbf{r})$  is a dimensionless function, which depends on the dielectric properties of the system and the ion distribution in the medium but not on the charge distribution within the protein. The function  $\chi_{\text{mp}}(\mathbf{r})$  has

the property that  $0 \leq \chi_{\text{mp}}(\mathbf{r}) \leq 1$  (Roux 1997). This function  $\chi_{\text{mp}}(\mathbf{r})$  describes how the membrane potential is modulated inside the membrane protein and can deviate from a simple linear function (Roux 1997).

The ions, protons and electrons that are transferred across the membrane are also influenced by the membrane potential. By analogy to the chemical potential  $\mu_c$  of a substance  $c$ , one can define the electrochemical potential  $\bar{\mu}_c$  for the ionic species  $c$  with charge  $z_c$  and activity  $\gamma[c]$  in a system with a membrane potential  $\Psi$ :

$$\bar{\mu}_c = \mu_c + z_c F \Theta(\mathbf{r}) \Psi \quad (6.45)$$

with

$$\mu_c = \bar{\mu}_c = \mu_c^\circ + RT \ln \gamma[c] \quad (6.46)$$

The energy for moving an ion across a membrane has thus two contributions: one arising from the work against the concentration difference between the two sides of the membrane and a second arising from work against the membrane potential  $\Psi$  (Cramer and Knaff 1991; Nicholls and Ferguson 2013). The work required to transfer an ion from one side of the membrane to the other is given by the difference between the electrochemical potential at the two sides of the membrane.

In order to account for the membrane potential in the energy calculation of a microstate, it is necessary to include the effect of the membrane potential on the binding energetics. Moreover, also the ligand concentrations on the two sides of the membrane may be different. Thus, a generalized version of Eq. 6.41 which uses binding free energies and electrochemical potentials instead of redox potentials,  $\text{p}K_a$  values and pH values defines the state energy for a transmembrane protein with  $N$  sites connected to the extracellular region (EC), and  $K$  sites connected to the cytoplasmic region (CP) (Calimet and Ullmann 2004; Bombarda et al. 2006) is

$$\begin{aligned}
G_n(\bar{\mu}_{c,i}^{\text{EC}}, \bar{\mu}_{h,j}^{\text{CP}}) &= \sum_{i=1}^N (x_i^n - x_i^\circ) (\bar{G}_{\text{intr},i}^\circ - \bar{\mu}_i^{\text{EC}}) \\
&+ \sum_{j=1}^K (x_j^n - x_j^\circ) (\bar{G}_{\text{intr},j}^\circ - \bar{\mu}_j^{\text{CP}}) \\
&+ \frac{1}{2} \sum_{i=1}^{N+K} \sum_{j=1}^{N+K} W_{ij} (x_i^n - x_i^\circ) (x_j^n - x_j^\circ)
\end{aligned} \tag{6.47}$$

where  $\bar{\mu}_i^{\text{EC}}$  and  $\bar{\mu}_j^{\text{CP}}$  are the electrochemical potentials of the ligand (for instance electrons or protons) binding to site  $i$  at the extracellular and site  $j$  at the cytoplasmic side, respectively. As before, the intrinsic binding energy ( $\bar{G}_{\text{intr},i}^\circ$ ) is the binding energy that the site  $i$  would have in the presence of a membrane potential if all the other titratable sites are in their reference state. The intrinsic binding energy  $\bar{G}_{\text{intr},i}^\circ$  has several contributions (For sites  $j$ , an analogous expression has to be used):

$$\bar{G}_{\text{intr},i}^\circ = G_{\text{model},i}^\circ + \Delta\Delta G_i^{\text{solv}} + \Delta\Delta G_i^{\text{back}} + \Delta\Delta G_i^\Psi \tag{6.48}$$

i.e., in addition to the terms in Eq. 6.28, Eq. 6.48 includes the interaction with the membrane potential  $\Delta\Delta G_i^\Psi$ , which can be obtained from

$$\begin{aligned}
\Delta\Delta G_i^\Psi &= F\Psi \Gamma_i \\
&= F\Psi \sum_{k=1}^{M_i} \chi_{\text{mp}}(\mathbf{r}_k) (Q_{k,i}^b - Q_{k,i}^u)
\end{aligned} \tag{6.49}$$

where the quantity  $\Gamma_i$  describes the relative effect of the membrane potential on the energy;  $\chi_{\text{mp}}(\mathbf{r})$  is the dimensionless function defined in Eq. 6.44;  $M_i$  is the number of charges of residue  $i$  that change during the reaction;  $Q_{k,i}^b$  and  $Q_{k,i}^u$  are the charges of atom  $k$  of residue  $i$  in the bound and unbound form, respectively.

It is important to realize that due to the membrane potential, there is an important

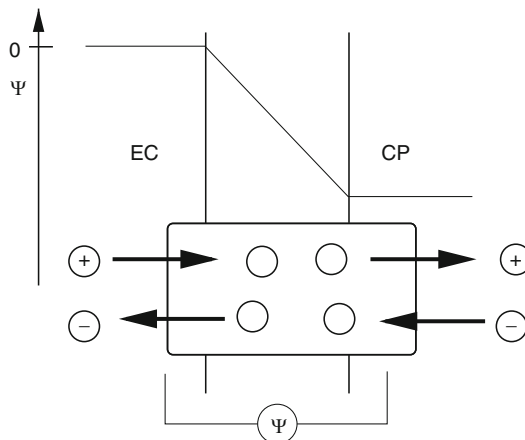


Fig. 6.9. Schematic representation of the ion, proton or electron flow in a membrane. In this scheme the membrane potential  $\Psi = \psi_{\text{CP}} - \psi_{\text{EC}} < 0$ , with  $\psi_{\text{CP}}$  and  $\psi_{\text{EC}}$  being the potential in the cytoplasm (CP) and in the extracellular space (EC), respectively. In case of protons, one could make the assumption that the hydrogen bond network connects the titratable sites to either the EC region or to the CP region (i.e. protons cannot flow through the protein). Proton displacement along one hydrogen bond network is favored in the direction of decreasing potential, electrons would flow in the opposite direction. Under the condition that the protons cannot pass the membrane, the membrane potential will increase the protonation probability of a titratable site receiving a proton from the EC region and it will decrease the protonation probability of a titratable site receiving a proton from the CP region. The opposite is true for electrons.

difference between the sites connected to the cytoplasm and the sites connected to the extracellular region (Bombarda et al. 2006). For example, a negative membrane potential as in Fig. 6.9 favors the protonation of sites connected to the extracellular side, since proton uptake is energetically downhill with regard to the membrane potential (Fig. 6.9). In contrast, protonation of sites connected to the cytoplasm is hindered in the presence of a negative membrane potential, since proton uptake is uphill with regard to the membrane potential (Bombarda et al. 2006). The opposite behavior will be found for electrons, i.e. the reduction from the extracellular side will be disfavored in the presence of a negative membrane potential, but favored from the cytoplasmic side.

## IV. Complex Electron Transfer Proteins

### A. Simulating Complex Electron Transfer Networks

To explore possible mechanisms of large protein complexes such as for instance the photosynthetic reaction center or also cytochrome *bc* complexes, it is often required to examine many different possibilities. Sometimes, even many mechanisms may be possible simultaneously and a single answer may not exist. Such complex reaction schemes can be investigated using the microstate model introduced in section “III.D. Interacting Redox Active Groups”. The kinetics of such reactions can be simulated by a master equation approach.

The rate constants which are required for such simulations can be calculated using the methods introduced above. Thus, combined with a master equation approach, continuum electrostatics offers a possibility to access the non-equilibrium behavior of biomolecular systems. In the microstate formalism, charge transfer events are described as transitions between well-defined microstates of a system. The time dependence of the population of each microstate can be simulated using a master equation

$$\frac{d}{dt}p_v(t) = \sum_{\mu=1}^M k_{v\mu}p_\mu(t) - \sum_{\mu=1}^M k_{\mu v}p_v(t) \quad (6.50)$$

where  $p_v(t)$  denotes the probability that the system is in charge state  $v$  at time  $t$ ,  $k_{v\mu}$  denotes the probability per unit time that the system will change its state from  $\mu$  to  $v$ . In Eq. 6.50, first sum includes all the reactions that form state  $v$ , the second sum includes all the reactions that annihilate state  $v$ . The summations run over all possible states  $\mu$ . Simulating charge transfer by Eq. 6.50 assumes that these processes can be described as a Markovian stochastic process. This assumption implies that the probability of a given charge transfer depends only on

the current state of the system and not on the pathway in which the system has reached this state. The system given by Eq. 6.50 is a system of coupled linear differential equations with constant coefficients, which can be written in the form

$$\frac{d\mathbf{p}(t)}{dt} = \mathbf{A}\mathbf{p}(t) \quad (6.51)$$

The diagonal element  $A_{vv}$  of the matrix  $\mathbf{A}$  is the negative of the sum over all the rate constants  $k_{\mu v}$  annihilating the state  $v$ . The off-diagonal element  $A_{v\mu}$  is the rate constant  $k_{v\mu}$  for the conversion of state  $\mu$  to state  $v$  (Becker et al. 2007). The analytical solution for such equations can be written as (Ferreira and Bashford 2006; Becker et al. 2007)

$$p_v(t) = \sum_{\mu}^M c_{\mu}v_{\mu,v}e^{-\alpha_{\mu}t} \quad (6.52)$$

where  $\alpha_{\mu}$  is the  $\mu$ th eigenvalue of the matrix  $\mathbf{A}$ , and  $v_{\mu,v}$  is the  $v$ th element of the  $\mu$ th eigenvector of matrix  $\mathbf{A}$ ;  $c_{\mu}$  are integration constants determined from the initial probabilities  $\mathbf{p}$  at  $t = 0$  (i.e. all the terms  $e^{\alpha_{\mu}t} = 1$ ).

$$\mathbf{c} = \mathbf{V}^{-1}\mathbf{p}(0) \quad (6.53)$$

where  $\mathbf{V}^{-1}$  is the inverse of the matrix containing the eigen vectors of  $\mathbf{A}$ .

Equation 6.52 describes the time dependence of the probability distribution of microstates of the system. For these microstates, energies  $G_v$  and transition probabilities  $k_{v\mu}$  can be assigned unambiguously. The time-dependent probability of finding a single site in a particular form can be obtained by summing up individual contributions from the time-dependent probabilities  $p_v(t)$ .

$$\langle x_i \rangle(t) = \sum_v^M x_{v,i}p_v(t) \quad (6.54)$$

If the reactions are electron transfer reactions, their rate constants can be estimated using, for example, the rate laws developed

by Moser and Dutton (Moser et al. 1992; Page et al. 1999) described in section “II.E. Moser-Dutton Ruler”.

### B. Analyzing Calculated Electron Transfer Networks

For the analysis of a complex charge transfer system, it is of particular interest to follow the flow of charges through the system, i.e., the charge flux. The flux from state  $\nu$  to state  $\mu$  is determined by the population of state  $\nu$  times the probability per unit time that state  $\nu$  will change into state  $\mu$ , i.e., by  $k_{\mu\nu}P_\nu(t)$ . The net flux between states  $\mu$  and  $\nu$  is thus given by

$$J_{\nu\mu}(t) = k_{\nu\mu}P_\mu(t) - k_{\mu\nu}P_\nu(t) \quad (6.55)$$

$J_{\nu\mu}$  (Eq. 6.55) is positive if there is a net flux from state  $\mu$  to state  $\nu$ . This flux analysis allows deduction of the reaction mechanism from even very complex reaction schemes (Becker et al. 2007).

In cases where the number of possible microstates is too large, the differential equation can not be solved analytically. Thus, approximations and simulations need to be applied. One attractive simulation is a dynamic Monte Carlo simulation scheme (Gillespie 2001; Till et al. 2008), which allows the simulation of very complex reaction mechanisms such as proton transfer through a protein matrix. Again, the reaction parameter can be obtained using simple approximations such as continuum electrostatics. Each simulation describes one particular reaction path through the possible states of the system. A reaction mechanism can then be inferred from the analysis of many such trajectories. Up to now, this method was only applied to relatively simple systems (Till et al. 2008). However, future application to enzymes which involve chemical transformation, proton and electron transfer, as well as conformational changes, seems possible and is a promising future road for analyzing enzyme functions.

### C. Electron Transfer from the C-Subunit of the Photosynthetic Reaction Center to the Special Pair

The microstate model described above has been used to simulate the kinetics of electron transfer between the tetraheme-subunit and the special pair of the photosynthetic reaction center of *Blastochloris viridis* (Becker et al. 2007; Bombarda and Ullmann 2011). The comparison with the experimental data (Ortega and Mathis 1993) shows that continuum electrostatic calculations can be used in combination with the empirical rate law of Eq. 6.12 to reproduce measurements on the re-reduction kinetics of the photo-oxidized special pair (SP) in the bacterial photosynthetic reaction center.

Re-reduction of the SP in *B. viridis* is facilitated by the cytochrome C-subunit

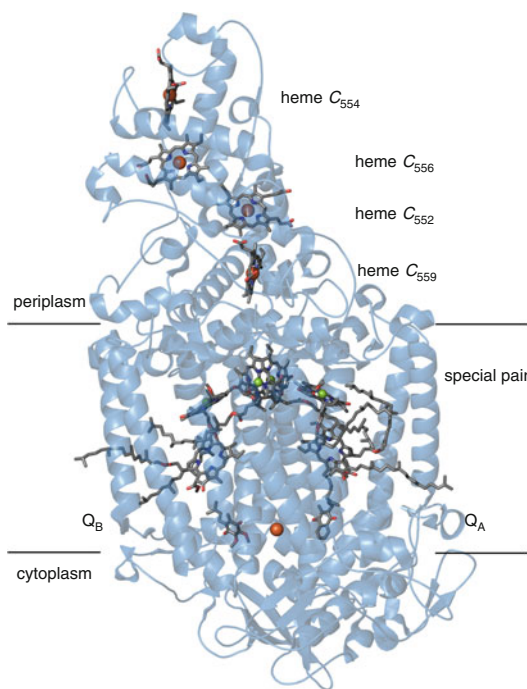


Fig. 6.10. Photosynthetic reaction center from *B. viridis*. In addition to the special pair, the accessory chlorophylls, the pheophytins and the quinones, this reaction center possesses four heme groups that re-reduce the special pair after photooxidation. The re-reduction kinetics of this protein has been well investigated experimentally.

(Fig. 6.10). The C-subunit, contains four heme cofactors forming a transfer chain. The heme groups are commonly labeled according to their absorbance maxima (subscripts) as heme  $c_{559}$ , heme  $c_{552}$ , heme  $c_{556}$  and heme  $c_{554}$ . To simulate electron transfer within the C-subunit and between the C-subunit and the SP, a model was constructed consisting of the five redox-active groups. Redox potentials of these groups and interaction energies for pairs of these groups were calculated using the model with pure electrostatic interaction. In addition, the available structural information was used to calculate reorganization energies for all different pairs of redox-active groups (Becker et al. 2007; Bombarda and Ullmann 2011).

In the experimental studies, Ortega et al. (1993) exposed the reaction center of *B. viridis* to different redox-potentials. The system was prepared experimentally in charge configurations with 4, 3 and 2 electrons distributed over the system consisting of the four hemes and the SP. The re-reduction kinetics of the SP was measured after photo-induced oxidation. These experimental setups can be mimicked by simulations. To illustrate the kinetics seen in such simulations, the result obtained for a system starting from 3 electrons distributed over the four heme groups is shown in Fig. 6.11. In Fig. 6.11a, the time-dependent probability distribution of the accessible microstates is shown. The corresponding oxidation probabilities for the hemes and the SP are shown in Fig. 6.11b. It can be seen that only a limited number of microstates contribute significantly to the probability distribution in the pico- to microsecond time domain. However, this feature does not imply that only this limited number of microstates is important for the kinetics of the system. The detailed information available from the simulation data allows to track the electron fluxes between microstates and thus electron movements between individual sites in a reaction scheme (Fig. 6.12).

The redox microstates can be denoted as vectors of 1 (reduced sites) and 0 (oxidized

sites). The first element denotes the redox state of the special pair, the next four elements denote redox states of the hemes in the order of their distance to the SP, starting from the nearest. The kinetics depicted in Fig. 6.11 suggests a rather simple picture for the time dependence of the population of accessible microstates. Starting from a population of the two microstates (0,1,1,1,0) (90%) and (0,1,0,1,1) (10%) after photooxidation, the system relaxes towards an equilibrium distribution which is mainly given by one microstate (1,1,0,1,0). However, the underlying transfer dynamics of the system as depicted in Fig. 6.12 is considerably more complex. The highly populated initial state (0,1,1,1,0) can rapidly decay into the final state via just one intermediate, (1,0,1,1,0). In contrast, the initial state (0,1,0,1,1) has to relax towards the final state via a succession of several intermediates. These intermediate states are only transiently populated. Each flux into one of the intermediates is accompanied by an equally high flux out of these intermediates. For example, the transition from the initial state to the intermediate (1,0,0,1,1) is rapidly followed by a transition to a second intermediate state (1,0,1,0,1). This intermediate state in turn either decays into state (1,0,1,1,0) via an electron transfer from heme  $c_{554}$  to heme  $c_{556}$ , or alternatively to state (1,1,0,0,1) via electron transfer from heme  $c_{552}$  to heme  $c_{559}$ .

The procedure outlined here can also be applied to proton transfer reactions. Thus, the strategy to combine continuum electrostatics with the master equation represents an important method to understand the mechanism of complex charge transfer systems.

## V. Conclusions

In this article, we reviewed how our understanding of the electron transfer in proteins on the basis of Marcus theory can help to analyze the mechanism of complex protein machines that can couple redox reactions to proton transfer reactions. Even the effect of membrane potentials and transmembrane



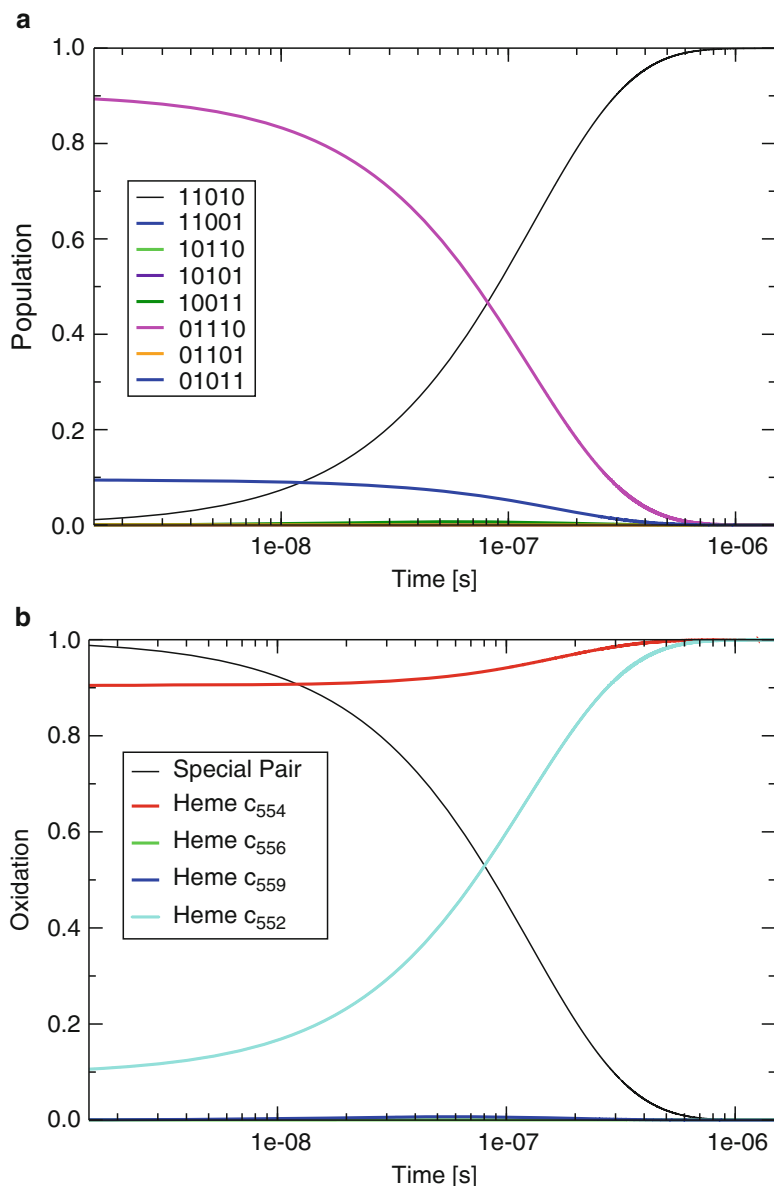


*Fig. 6.11.* Simulation of the re-reduction kinetics of the special pair of the photosynthetic reaction center in a system with three electrons. (a) The time-dependent probability distribution of microstates after photo-oxidation of the SP. The state vector is given in the order (SP, heme  $c_{559}$ , heme  $c_{552}$ , heme  $c_{556}$ , heme  $c_{554}$ ). In the state vector, 1 denotes a reduced site and 0 an oxidized site. States that are not shown are not significantly populated. (b) Oxidation probabilities of the four hemes and the SP. Initially, three electrons are distributed over the four hemes.

concentration gradients can be included in the calculations. The theoretical basis of the analysis of complex protein machines is the microstate model. In this model, the protein is divided into several functional groups, which can be, for instance, redox-

active centers (like hemes or iron sulfur clusters), protonatable residues (like histidine or glutamate), or enzymatic active sites. The part of the protein that does not belong to a functional group is considered a background that interacts with the functional groups.

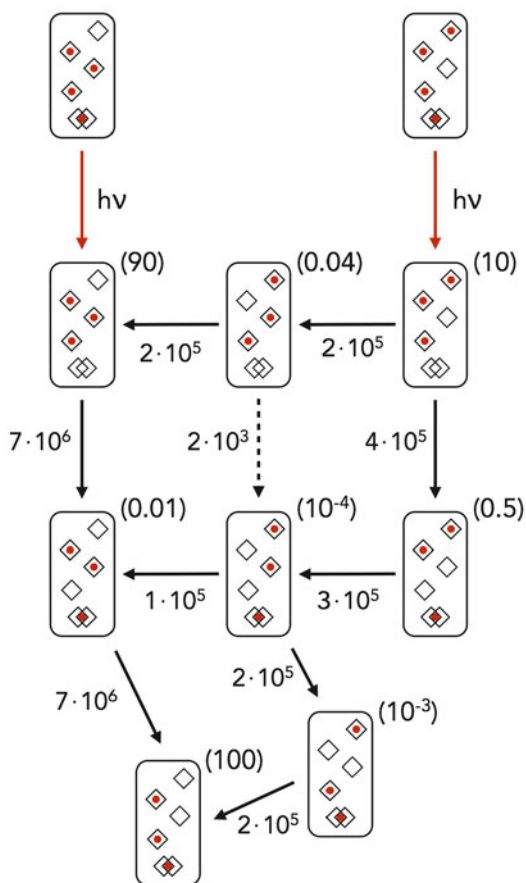


Fig. 6.12. Reaction scheme for the rereduction kinetics of the special pair of the photosynthetic reaction center in a system with three electrons. The reaction scheme is deduced from the flux analysis. Each *rectangle* represents a microstate of the photosynthetic reaction center, the *rhombi* inside the *rectangle* represent the hemes (the order top to bottom: heme  $c_{554}$ , heme  $c_{556}$ , heme  $c_{552}$ , heme  $c_{559}$ ), the overlapping *rhombi* represent the special pair. The reduced state of the cofactors is indicated by a *red sphere*. After photooxidation of the special pair (*red arrows*), several electron transfer reactions lead to the new equilibrium. The microstates representing the starting and the final configurations of the system in the simulation are depicted in the top and the bottom row, respectively. The values in parentheses denote the maximal probability observed during the simulation. Only fluxes (in  $s^{-1}$ ) contributing significantly are indicated by *arrows* and their maximum value is given.

The state of the protein is characterized by defining the state of each functional group (for instance redox state or protonation state). In this picture, a protein with  $N$  sites has many states (precisely  $\prod_{i=1}^N s_i$ , where  $s_i$  is the number of states of site  $i$ ). The energy of a particular state is defined by the sum of the energies of each particular site and the interactions between the sites. In this energy sum, the interaction with membrane potentials or other external fields can also be included.

Thermodynamic properties can be calculated by averaging over all possible states of the systems using statistical thermodynamics. If the system has so many states that explicit averaging is not possible, Metropolis Monte Carlo can be applied. To simulate the kinetic behavior of the protein, a master equation including all transitions between the states can be used. A flux analysis can help to extract mechanistic information from the simulation.

The microstate model is fairly general and does not rely on any particular way by which the state energies or the transition rate constants are calculated. In this article, we showed that the use of continuum electrostatic theory on the basis of the Poisson-Boltzmann equation is particularly useful, since, even for very large systems, the calculations are still tractable and lead to biophysically and biochemically meaningful results. The energies and rate constants of the microstate model could also be calculated with more accurate methods. However, it is important to realize that proteins that contain many cofactors cannot be regarded as a sum of these cofactors. Instead such proteins can exist in many states. Which states are functionally important, for instance, in catalytic cycles can be revealed by the analysis described in this article. We are convinced that the methods described here will allow analysis of many complex enzymatic reactions.

## Acknowledgements

This work was supported by the DFG RTG 1640 (Photophysics of Synthetic and Biological Multichromophoric Systems) and by the DFG Grant BO 3578/1.

## References

- Banerjee R (2008) Redox biochemistry. Wiley, Hoboken
- Bashford D, Karplus M (1990)  $pK_a$ s of ionizable groups in proteins: atomic detail from a continuum electrostatic model. *Biochemistry* 29:10219–10225
- Becker T, Ullmann RT, Ullmann GM (2007) Simulation of the electron transfer between the tetraheme-subunit and the special pair of the photosynthetic reaction center using a microstate description. *J Phys Chem B* 111:2957–2968
- Beroza P, Fredkin DR, Okamura MY, Feher G (1991) Protonation of interacting residues in a protein by a Monte Carlo method: application to lysozyme and the photosynthetic reaction center. *Proc Natl Acad Sci USA* 88:5804–5808
- Beveridge DL, DiCapua FM (1989) Free energy via molecular simulation: applications to chemical and biomolecular systems. *Ann Rev Biophys Biochem* 18:431–492
- Bombarda E, Ullmann GM (2011) Continuum electrostatic investigations of charge transfer processes in biological molecules using a microstate description. *Faraday Discuss* 148:173–193
- Bombarda E, Becker T, Ullmann GM (2006) The influence of the membrane potential on the protonation of bacteriorhodopsin: insights from electrostatic calculations into the regulation of proton pumping. *J Am Chem Soc* 128:12129–12139
- Born M (1920) Volumen und Hydratationswärme der Ionen. *Z Physik* 1:45–48
- Calimet N, Ullmann GM (2004) The influence of a transmembrane pH gradient on protonation probabilities of bacteriorhodopsin: the structural basis of the back-pressure effect. *J Mol Biol* 339:571–589
- Connolly M (1983) Solvent-accessible surfaces of proteins and nucleic acids. *Science* 221:709–713
- Cramer WA, Knaff DB (1991) Energy transduction in biological membranes. Springer, New York
- Crofts AR, Rose S (2007) Marcus treatment of endergonic reactions: a commentary. *Biochim Biophys Acta* 1767:1228–1232
- Crofts AR (2004) The cytochrome bc1 complex: function in the context of structure. *Ann Rev Physiol* 66:689–733
- da Silva JF, Williams R (2001) The biological chemistry of the elements – the inorganic chemistry of life. Oxford University Press, New York
- Davidson VL (2007) Protein-derived cofactors. Expanding the scope of post-translational modifications. *Biochemistry* 46:5283–5292
- Deponce M (2013) Glutathione catalysis and the reaction mechanisms of glutathione-dependent enzymes. *Biochim Biophys Acta* 1830:3217–3266
- Ferreira A, Bashford D (2006) Model for proton transport coupled to protein conformational change: application to proton pumping in the bacteriorhodopsin photocycle. *J Am Chem Soc* 128:16778–16790
- Gamow G (1928) Zur Quantentheorie des Atomkernes. *Z Physik* 51:204–212
- Gillespie DT (2001) Approximate accelerated stochastic simulation of chemically reacting systems. *J Chem Phys* 115:1716–1733
- Gray HB, Winkler JR (1996) Electron transfer in proteins. *Annu Rev Biochem* 65:537–561
- Gray HB, Winkler JR (2005) Long-range electron transfer. *Proc Natl Acad Sci USA* 102:3534–3539
- Gunner MR, Mao J, Song Y, Kim J (2006) Factors influencing the energetics of electron and proton transfers in proteins. What can be learned from calculations. *Biochim Biophys Acta* 1757:942–968
- Honig B, Nicholls A (1995) Classical electrostatics in biology and chemistry. *Science* 268:1144–1149

- Logan BE (2008) Microbial fuel cells. Wiley, Hoboken
- Marcus RA, Sutin N (1985) Electron transfer in chemistry and biology. *Biochim Biophys Acta* 811:265–322
- Marcus RA (1956) On the theory of oxidation-reduction reactions involving electron transfer. *J Chem Phys* 24:966–978
- Martin W, Baross J, Kelley D, Russell MJ (2008) Hydrothermal vents and the origin of life. *Nat Rev Microbiol* 6:805–814
- Mitchell P (1961) Coupling of phosphorylation to electron and hydrogen transfer by a chemi-osmotic type of mechanism. *Nature* 191:144–148
- Mitchell P (1976) Possible molecular mechanisms of the protonmotive function of cytochrome systems. *J Theor Biol* 62:327–367
- Moser CC, Keske JM, Warneke K, Farid RS, Dutton PL (1992) Nature of biological electron transfer. *Nature* 355:796–802
- Muegge I, Qi PX, Wand AJ, Chu ZT, Warshel A (1997) The reorganization energy of cytochrome *c* revisited. *J Phys Chem B* 101:825–836
- Nicholls DG, Ferguson S (2013) Bioenergetics, 4th edn. Elsevier, Amsterdam
- Nielsen JE, McCammon JA (2003) Calculating pKa values in enzyme active sites. *Protein Sci* 12:1894–1901
- Olsson MHM, Ryde U, Roos BO (1998) Quantum chemical calculation of the reorganization energy of blue copper proteins. *Prot Sci* 81:6554–6558
- Onufriev A, Case DA, Ullmann GM (2001) A novel view on the pH titration of biomolecules. *Biochemistry* 40:3413–3419
- Ortega JM, Mathis P (1993) Electron transfer from the tetraheme cytochrome to the special pair in isolated reaction centers of *Rhodospseudomonas viridis*. *Biochemistry* 32:1141–1151
- Page CC, Moser CC, Chen X, Dutton PL (1999) Natural engineering principles of electron tunneling in biological oxidation-reduction. *Nature* 402:47–52
- Pedersen A, Karlsson GB, Rydström J (2008) Proton-translocating transhydrogenase: an update of unsolved and controversial issues. *J Bioenerg Biomemb* 40:463–473
- Roux B (1997) The influence of the membrane potential on the free energy of an intrinsic protein. *Biophys J* 73:2981–2989
- Ryde U, Olsson MHM (2001) Structure, strain and reorganization energy of blue copper models in the protein. *Int J Quant Chem* 81:335–347
- Sharp KE (1998) Calculation of electron transfer reorganization energies using the finite difference poisson-Boltzmann model. *Biophys J* 73:1241–1250
- Stubbe J, van der Donk WA (1998) Protein radicals in enzyme catalysis. *Chem Rev* 98:705–776
- Stuchebrukhov A (2003) Long-distance electron tunneling in proteins. *Theor Chem Acc* 110:314–344
- Till MS, Becker T, Essigke T, Ullmann GM (2008) Simulating the proton transfer in Gramicidin A by a sequential dynamical Monte Carlo method. *J Phys Chem B* 112:13401–13410
- Ullmann GM, Bombarda E (2013) pK(a) values and redox potentials of proteins. What do they mean? *Biol Chem* 394:611–619
- Ullmann GM, Knapp EW (1999) Electrostatic computations of protonation and redox equilibria in proteins. *Eur Biophys J* 28:533–551
- Ullmann GM, Kostić NM (1995) Electron-tunneling paths in various electrostatic complexes between cytochrome *c* and plastocyanin. Anisotropy of the copper-ligand interactions and dependence of the iron-copper electronic coupling on the metalloprotein orientation. *J Am Chem Soc* 117:4766–4774
- Ullmann RT, Ullmann GM (2012) GMCT: a Monte Carlo simulation package for macromolecular receptors. *J Comput Chem* 33:887–900
- Ullmann GM, Kloppmann E, Essigke T, Krammer EM, Klingens AR, Becker T, Bombarda E (2008) Investigating the mechanisms of photosynthetic proteins using continuum electrostatics. *Photosynth Res* 97:33–53
- Ullmann GM (2000) The coupling of protonation and reduction in proteins with multiple redox centers: theory, computational method, and application to cytochrome *c*<sub>3</sub>. *J Phys Chem B* 104:6293–6301
- Ullmann GM (2003) Relations between protonation constants and titration curves in polyprotic acids: a critical view. *J Phys Chem B* 107:6293–6301
- Warren JJ, Winkler JR, Gray HB (2012) Redox properties of tyrosine and related molecules. *FEBS Lett* 586:596–602
- Warwicker J, Watson HC (1982) Calculation of the electrostatic potential in the active site cleft due to the  $\alpha$ -helix dipoles. *J Mol Biol* 186:671–679
- Wessjohann LA, Schneider A, Abbas M, Brandt W (2007) Selenium in chemistry and biochemistry in comparison to sulfur. *Biol Chem* 388:997–1006
- Wilson GS (1983) Electrochemical studies of porphyrin redox reactions as cytochrome models. *Bioelectrochem Bioenerg* 1:172–179
- Woycechowsky K, Raines R (2000) Native disulfide bond formation in proteins. *Curr Opin Chem Biol* 4:533–539

- You T, Bashford D (1995) Conformation and hydrogen ion titration of proteins: a continuum electrostatic model with conformational flexibility. *Biophys J* 69:1721–1733
- Zhang Z, Huang L, Shulmeister VM, Chi YI, Kim KK, Hung LW, Crofts AR, Berry EA, Kim SH (1998) Electron transfer by domain movement in cytochrome bc<sub>1</sub>. *Nature* 392:677–684
- Zheng Z, Gunner MR (2009) Analysis of the electrochemistry of hemes with E(m)s spanning 800 mV. *Proteins* 75:719–734
- Zhou M, Wang H, Hassett DJ, Gu T (2013) Recent advances in microbial fuel cells (MFCs) and microbial electrolysis cells (MECs) for wastewater treatment, bioenergy and bioproducts. *J Chem Tech Biotech* 88:508–518